



Trinity College Dublin
Coláiste na Tríonóide, Baile Átha Cliath
The University of Dublin

The inner blood retinal barrier in ocular disease and circadian regulation: its role in age related macular degeneration development and other neuro-ophthalmology disorders

A thesis presented for the Master of Science degree 2023

Smurfit Institute of Genetics, Trinity College Dublin

By

Fionn O'Leary

MB, BCh, BAO, BSc

Supervisor: Dr Matthew Campbell

Associate Professor

Neurovascular Genetics Laboratory

Trinity College Dublin



Trinity College Dublin
Coláiste na Tríonóide, Baile Átha Cliath
The University of Dublin

Declaration:

I declare that this thesis has not been submitted as an exercise for a degree at this or any other university and it is entirely my own work.

I agree to deposit this thesis in the University's open access institutional repository or allow the library to do so on my behalf, subject to Irish Copyright Legislation and Trinity College Library conditions of use and acknowledgement.

I consent to the examiner retaining a copy of the thesis beyond the examining period, should they so wish.

Fionn O'Leary

July 2022



Trinity College Dublin
Coláiste na Tríonóide, Baile Átha Cliath
The University of Dublin

Acknowledgements:

I wish to express my gratitude and thanks to Dr. Matt Campbell for his help, support, patience, and invaluable feedback throughout the year. In addition, this project would not have been possible without the time, expertise, and guidance of Mr. Mark Cahill.

I am also grateful to Dr. Natalie Hudson and Dr. Jeffrey O’Callaghan for their substantial input and help with this project. As many know, academic research is both an individual and team effort, and I sincerely thank you both for your advice and support.

Lastly, I would like to thank those close to me who have stood by and supported me through this year and previous.



Trinity College Dublin
Coláiste na Tríonóide, Baile Átha Cliath
The University of Dublin

Abstract:

Age related macular degeneration (AMD) is one of the most common causes of irreversible sight loss worldwide. The initial pathophysiological events that occur in AMD are poorly understood, with most research focusing on the outer blood retinal barrier (oBRB), choroid and RPE dysfunction. This research is focused on circadian regulation of inner blood retinal barrier (iBRB) permeability, and how dysfunction of this barrier may be one of the initiating events in photoreceptor/RPE stress and AMD development. There is a gap in knowledge of the disease process and an unmet need for an effective therapeutic agent that can target these aberrant processes at an early stage of disease. The tight junction (TJ) protein claudin-5, which cycles in a circadian manner, is thought to be central to the maintenance of iBRB integrity.

Fluorescein signal at the macula can act as a proxy for iBRB integrity. Previous work has shown that there is a circadian associated fluorescein signal differential present in young healthy controls under 30 years. An increased fluorescein signal at the macula is present in the evening compared to the morning in this group. Results from this research show this is not present in age matched controls and AMD participants suggesting that the circadian dependant iBRB kinesis present in younger people may decrease with ageing and may be further decreased or arrested fully in AMD. We believe this may be one of the early initiating factors in AMD pathogenesis. A more permanently open or “leaky” iBRB may contribute to increased photoreceptor/RPE stress and commence the cycle of pathophysiological events leading to AMD development.

Claudin-5 is the dominant TJ protein not only in the iBRB but also in the blood brain barrier (BBB). Some neurological diseases have demonstrated abnormal and increased BBB permeability. It follows therefore due to the molecular similarities between the BBB and iBRB, dysfunction in iBRB permeability may also be evident in these conditions. The healthy young control dataset from the IRCP allows a comparison between iBRB permeability in these neurological conditions and healthy controls.

Visual Snow (VS) syndrome is a condition defined by the subjective reporting of constant positive visual phenomenon or “static background” in both eyes. No assessment of the iBRB is evident in the literature. We therefore carried out ocular assessment and imaging of participants with VS symptoms. We have observed an increased permeability of the iBRB when compared to healthy young controls.

In conclusion, the iBRB permeability is highly dynamic in many conditions including AMD and VS, and that abnormal permeability may be a significant factor in the pathogenesis of these conditions. Studies have also begun investing the role of the iBRB in other neuro ophthalmology conditions such as Tuberous Sclerosis, traumatic brain injury and other rare neurological conditions.



TABLE OF CONTENTS

DECLARATION	2
ACKNOWLEDGMENTS	3
ABSTRACT.....	4
1. INTRODUCTION	
1.1 The blood retinal barrier (BRB).....	6
1.2 The BRB in age related macular degeneration.....	9
1.3 Circadian rhythms.....	11
1.4 The blood brain barrier (BBB) and BRB similarities.....	12
1.5 Visual Snow Syndrome.....	13
1.6 Aims and Objectives.....	14
2. METHODOLOGY	
2.1 The AMD Irish Retinal Circadian project (IRCP).....	15
2.2 Fluorescent Ocular Analysis Software.....	18
2.3 Visual Snow Syndrome.....	20
3. RESULTS	
3.1 The AMD Irish Retinal Circadian project (IRCP)	21
3.1.1 Sample participant images.....	21
3.1.2 Healthy young control data.....	25
3.1.3 Age matched control data.....	27
3.1.4 AMD data.....	29
3.1.5 Healthy young control vs AMD data.....	32
3.2 Visual Snow Syndrome	34
3.2.1 Participant images.....	34
3.2.2 VS data vs healthy young control data.....	39
4. DISCUSSION AND CONCLUSION	
4.1 The AMD IRCP.....	46
4.2 VS.....	51
REFERENCES	54
APPENDICES	
A. The Munich Chronotype Questionnaire (MCTQ).....	59
B. Participant Health Questionnaire.....	60

INTRODUCTION

1.1 The Blood Retinal Barrier (BRB)

The retina, a portion of the central nervous system and in effect an extension of the brain, has the highest oxygen consumption per unit weight of any tissue in the body. This environment along with high metabolic demand makes the retina, and particularly the macula, susceptible to oxidative stress causing damage to central vision [1]. Therefore, the microenvironment of the retina must be tightly regulated, and is separated from the systemic circulation by the blood retina barrier (BRB). More specifically, the inner blood retina barrier (iBRB) is used to describe the properties of the endothelial cells and their tight junction (TJ) proteins that line the microvasculature of the inner retina, while the outer blood retina barrier (oBRB) refers to the properties of the retinal pigment epithelium (RPE) cells which separate the fenestrated choriocapillaris from the retina [2, 3].

The oBRB consists of the choroid, Bruch's membrane and the RPE. The choroid from outer to inner portions consists of the suprachoroid, large and medium blood vessel layer, and the choriocapillaris [2]. The choriocapillaris contains fenestrations and is actively involved in the supply of nutrients and removal of waste material from the outer retinal layers, including the RPE and photoreceptors (PRs) [4]. BM is located between the choriocapillaris basement membrane and the RPE basement membrane and consists of outer and inner collagenous layers separated by a central elastic layer [5]. The BM allows for the size selective passive diffusion of molecules through it, blocking large molecule diffusion [6]. Other functions include prevention of inflammatory cell migration, stabilisation of the RPE layer, and absorption of physical stress forces [7].

Specifically related to the oBRB, the RPE is a modified neuroepithelial cell. The RPE is a single layer of hexagonal, polarised, pigment containing cells which directly underlie the neural retina. The TJs of the RPE are located at the apical surface and are mainly responsible for maintaining oBRB integrity [8]. Numerous microvilli extend from the apical surface of the RPE and surround the photoreceptor outer segments (POS) increasing the surface area in contact with POS approximately 30-fold, thereby promoting increased cellular contact and regulation [9]. Stimulation of PRs by light results in the accumulation of photo-damaged molecules and free radical production, the majority of which occur in the POS. The POS is shed daily and phagocytosed by RPE cells, with new POS forming at the cilium at the base of outer segments [8, 9]. Phagocytosis is controlled by the circadian rhythm, mostly occurring in the early morning [9]. The RPE also contributes to the recycling of essential digested POS molecules, such as vitamin A, back to PRs along with retinoid storage and conversion, crucial to the visual cycle [8, 9].

The RPE secretes several molecules and growth factors, such as pigment epithelial cell derived factor and vascular endothelial growth factor (VEGF), which help maintain retinal and choriocapillaris structural integrity [10]. VEGF secreted at the basolateral surface of the RPE stabilises the choriocapillaris by preventing apoptosis and maintains fenestrations of endothelial cells [9, 11]. Melanin granules are located mostly near the apical surface and absorb scattered and out of focus light, which helps maintain clear vision [9].

The second barrier system of the retina is the iBRB. This barrier is composed of endothelial cells that line the retinal vasculature which originates from the central retinal artery and

supplies the inner retinal layers. The vasculature penetrates the retina at three main plexuses: the superficial, intermediate, and deep layers which correspond to the nerve fibre layer, inner plexiform layer, and outer plexiform layer respectively [12]. The PR layer of the retina is avascular [3]. See Figure 1 for comparison of the iBRB and oBRB.

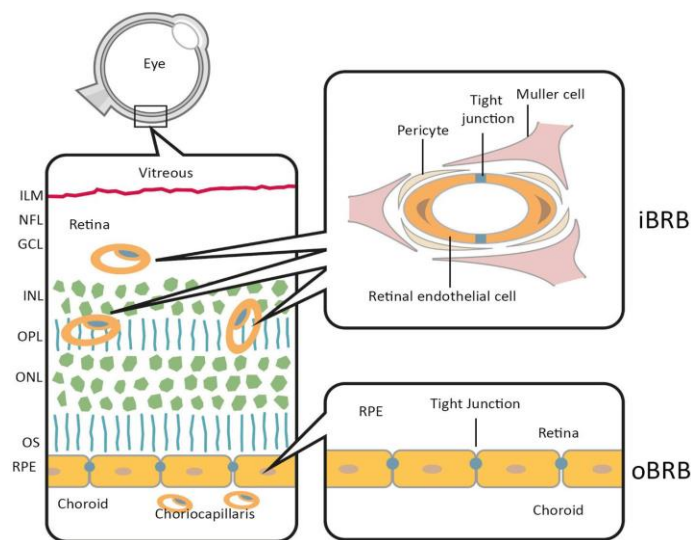


Figure 1: The iBRB and oBRB

Source: O’Leary F, Campbell M. The blood–retina barrier in health and disease. *The FEBS Journal*. 2021 Dec 18.

The neurovascular unit (NVU)

While the iBRB refers to the unique properties of the retinal endothelial cells, the general make-up of the iBRB consists of the neurovascular unit (NVU), which is similar in structure and function to the blood brain barrier (BBB) [13]. The retinal NVU comprises the retinal vascular endothelial cells with their dual basement membrane, surrounded by pericytes and glial cells including astrocytes, Müller cells and microglia [13, 14].

The NVU contributes to the overall integrity of the iBRB. Retinal pericytes which contribute heavily to this integrity, are contractile, phagocytic cells embedded in the capillary basement membrane with a higher ratio in the retina compared to any other tissue in the body [15]. They stabilise the microvasculature, regulate blood flow, and can control endothelial cell proliferation, and thus have a role in angiogenesis [14]. They can further regulate the retinal microenvironment by secretion of extracellular matrix components such as fibronectin [14, 16]. Astrocytes which are predominately located in the nerve fibre and inner nuclear layers, can modulate the BRB by releasing trophic factors, antioxidants, and both pro- and anti-inflammatory cytokines to the NVU microenvironment [17, 18]. Their processes surround retinal vascular endothelial cells which leads to a more intact TJ barrier [17, 19]. High glucose disrupts astrocyte function, morphology, and TJ integrity [19].

Müller cells located throughout all layers of the retina, interact via their foot processes at synapses with other neuronal cells in the retina (including ganglion, bipolar and amacrine cells) [17, 20]. Their footplates form the internal limiting membrane and surround blood vessels providing a further support function [17, 20]. Through these interactions they have been shown

to release vasoactive substances, so called “gliotransmitters” and thus modulate neuron transmission and endothelial cell permeability [17, 20].

Microglia are resident glial macrophages which are predominately located close to the retinal vasculature where they can clear cellular and metabolic debris [13]. Despite the relative immune privilege of the eye, microglia become activated in an inflammatory environment, release proinflammatory molecules and undertake phagocytosis [13]. In addition to their proinflammatory immune function, they also interact and secrete biochemical factors which influence neuronal transmission, synaptic plasticity, and other cells in the NVU [17, 20].

Retinal endothelial cells

Retinal endothelial cells and their TJs are the key contributors to the iBRB. They function to protect the sensitive neurosensory retina from the systemic circulation, including from microorganisms, proinflammatory cells and toxins [79]. On the other hand, they must also allow some transport of molecules and cells across the endothelium, to supply the highly metabolically active retinal tissue [79]. The retinal microenvironment is heavily reliant on autoregulation, and the retinal endothelial cells play a key role by regulating the tone of retinal arterioles and stimulating vasoconstriction and vasodilation by sensing changes in the microenvironment such as hypercapnia, hypoxia, or acidosis [80]. This is achieved through the release of chemicals such as nitric oxide and arachidonic acid derivatives [80].

The glycocalyx, a proteoglycan rich layer located on the apical surface of retinal endothelium cells, is also a major contributor to autoregulation of retinal blood flow [81]. However, it also plays other key roles in iBRB maintenance including repelling charged molecules and cells away from the endothelium, regulating the movement of fluid between blood and the interstitial space, and limits the effect of shear stress on endothelial cells [82]. Retinal endothelial cells also lack fenestrations and have a high presence of intercellular junction proteins known as zonula occludens. These, in addition to claudins, are a key contributor to stable “tight” TJs, which greatly limit paracellular diffusion [80].

In addition, the tight control of transcellular transport of molecules through the interstitium of the retinal endothelium is also very important in iBRB maintenance [75]. In fact, the retinal endothelium contains a much lower level of transcytosis and receptor mediated transport compared to other endothelium in the body and a higher level of efflux pumps, which move ions and fluid across the endothelium, helping to maintain the optimum conditions in the retinal microenvironment [82].

Transcellular transport is tightly regulated, mostly through decreased expression of vesicle forming proteins such as caveolae (areas of invaginations in the plasma membrane which consist of lipid rafts and other proteins) relative to other endothelial tissues [83]. Major Facilitator Superfamily Domain Containing 2A (*mfsd2a*), a transmembrane protein and the main inhibitor of caveolae-mediated vesicle formation and transcytosis, is highly expressed in retinal endothelium [84]. In many retinal diseases including neovascular AMD and diabetic retinopathy, increased levels of VEGF play a major role in BRB breakdown and pathogenesis. The rate of caveolae-mediated endocytosis has been shown to increase (and thus the permeability of the iBRB) in an increased VEGF environment [85].

Tight junction proteins

In addition to the properties of the retinal endothelium cells, TJs serve as the key barrier components in both the iBRB and BBB. TJ proteins project inwards and interact in the paracellular space creating a “barrier” effect [21]. They consist predominantly of the claudin family proteins, MARVEL family transmembrane proteins, and junctional adhesion molecules (JAMs). TJs of endothelial cells are more structurally complex, dispersed between and frequently interacting with gap and adherens junctions, as tight regulation of vascular permeability is required [22]. Retinal endothelial cells have the smallest intercellular space and the highest number of TJ strands in comparison to any other tissue containing endothelial cells [23].

Claudins are likely the most important proteins in TJ formation, cell-cell adhesion, and regulation of TJ permeability as they facilitate passive diffusion by forming pores in the paracellular space [24, 25]. At the iBRB and BBB, claudin-5 is the most highly expressed claudin protein and indeed the highest expressed TJ component [26, 27]. Its levels are critical in maintaining retinal homeostasis, as blood vessels of claudin -5 deficient mice are more permeable to molecules less than 800 Da [26]. After birth, claudin-5 KO mice die within 10 hours and display profound BBB leakiness to molecules <800 Da [26]. Other studies modelling ischemia and diabetes demonstrate that claudin-5 loss is the main driver of increased BBB and iBRB permeability, thus further indicating claudin-5’s importance in supporting the BBB and iBRB [28, 29]. Most evidence suggests that it is the breakdown of the TJ complexes between endothelial cells which contributes to iBRB breakdown and subsequent retinal oedema that is observed as a feature in numerous retinal conditions [14, 22, 24].

1.2 The BRB in age related macular degeneration (AMD)

AMD is the number one cause of retinal blindness worldwide with the incidence expected to continue to increase [30]. AMD results in irreversible loss of central vision due to retinal degeneration in the macula, the cone rich central portion of the retina [31]. Risk factors include cigarette smoke, alcohol, Western style diet, aging and genetic polymorphisms (e.g., complement factor H and the ARMS2 variants) all of which contribute to increased oxidative stress thought to be the central mechanism leading to PR/RPE dysfunction and BRB breakdown [32].

AMD can be classified into two types “dry” and “wet”. AMD in its early stages is generally asymptomatic and can be identified during clinical examination of the retina by yellowish deposits known as drusen in the subretinal or sub-RPE regions [31]. RPE dysfunction, loss and PR death can progress at the macula resulting in the end stage of “dry” AMD termed geographic atrophy (GA) [30, 31]. GA typically affects the perifoveal region first, before gradually enlarging and coalescing to affect the fovea. Therefore, good visual acuity is often present due to foveal sparing [33]. “Wet” AMD has a faster progression, occurs in approximately 10% of cases and is characterised by choroidal neovascularisation (CNV), where the underlying choroid neovascularises which leads to haemorrhage, oedema and ultimately PR cell death [30, 31]. Increased levels of VEGF are the main driver of CNV formation, therefore anti-VEGF intravitreal injections are an effective treatment option for “wet” AMD [34]. There are no treatments currently available for GA secondary to “dry” AMD. However, the use of low vision

aids and lifestyle modifications, such as smoking cessation, dietary changes, and supplementation (e.g., macushield) are recommended. The Age-Related Eye Disease Study (AREDS) demonstrated a 25% risk reduction in progression of categories 3 (1 large druse) and 4 (advanced) AMD in patients receiving antioxidants (Vitamin C, E, and beta-carotene) and zinc versus the placebo group [35].

The projected increased incidence of AMD, in addition to the significant effects on patient's vision and quality of life requires an increased understanding of the underlying causes and initiating events of the disease. Some of the molecular mechanisms present in the disease course are described below, but the specific order of events and initiating steps remain elusive.

Pathophysiology

In early AMD, RPE function begins to decline due to oxidative stress, the development of reactive oxygen species and the accumulation of undigested material known as lipofuscin [36]. The major risk factors of AMD (age, genetic polymorphisms, cigarette smoke etc.) are known to contribute to oxidative stress [32]. Thus, the recommendation for the use of natural antioxidant supplementation from the AREDS [35]. In aging and AMD, oxidative stress increases due to a decrease in the natural antioxidant defence mechanisms in the retina including antioxidant enzymes (catalases and superoxide dismutases), Nuclear factor erythroid-2 related factor 2 (Nrf2) transcription factor levels, impairment of autophagy, and increased levels of apoptosis events [91].

In later stages, RPE cells lose their unique hexagonal morphology and functions [37]. Recently, this loss of cell differentiation, known as epithelial-mesenchymal transition, has been shown to result in multinucleation, loss of TJs and loss of RPE morphology, all contributing to oBRB loss, dysregulated gas and molecule exchange and further RPE/PR damage [37]. The build-up of waste material and thickening with calcification of BM leads to impaired diffusion of nutrients and oxygen along with impaired removal of waste material between the RPE and choriocapillaris [38]. This can further damage the retina and RPE cells, leading to further oBRB integrity loss [38]. Decreased choroidal thickness and reduced choriocapillaris vascularity are also features of AMD. This likely leads to decreased oxygen and nutrient supply to the RPE, adding further metabolic stress to RPE cells and contributing to oBRB breakdown [39, 40].

This traditional line of thought suggests that dysfunction in the RPE and the choriocapillaris as the primary sites of AMD pathogenesis, as outlined above. This research hypothesises that abnormal inner retinal vasculature permeability (particularly the loss of circadian regulation of this permeability) may be the primary reason for AMD disease development with secondary RPE and choriocapillary dysfunction as a result.

The iBRB in AMD

Early indications that the iBRB may be involved in AMD progression and GA development came from macular translocation studies by *Cahill et al*[44]. Here, patients with GA underwent surgery involving movement of the area of retina and RPE with GA inferiorly away from the macula, with healthy peripheral neurosensory retina translocated to the macula, thus helping to improve central vision [44]. However, at 12 months post operatively a new area of GA was seen developing at the macula despite the presence of new neurosensory retina translocation to this area 12 months previously, suggesting the presence of disease process in the inner retinal layers compared to outer [44].

Some earlier studies have also provided evidence for dysfunction of the iBRB in AMD. Post-mortem analysis of human donor eyes with dry AMD revealed increased levels of plasma proteins such as fibrinogen, albumin, complement, and immunoglobulins indicating iBRB breakdown may also be a key element of AMD progression [41]. This iBRB breakdown can result in loss of immune privilege and subsequent inflammatory cascade with neural retina injury [42]. Indeed, it has also been shown in mouse, non-human primates, and human subjects, that the iBRB is highly dynamic and appears to be regulated by the circadian clock. The key iBRB associated TJ protein claudin-5 cycles in a circadian manner and it is thought that its dysregulation may be a key driver of the early stages of dry AMD [43].

1.3 Circadian rhythms

The role of the circadian rhythm on iBRB physiology is an essential aspect of this study. The human circadian clock is in the hypothalamus, specifically in the suprachiasmatic nucleus (SCN) [45]. It is the master regulator controlling approximately a 24-hour sleep-wake cycle, whilst also controlling aspects of hormone regulation such as melatonin and cholesterol, eating and fasting, and body temperature [45]. Light is the most important element that “resets” the circadian clock, where signals from retinal ganglion cells reach the SCN [46].

Decreased TJ expression of proteins such as claudin-5 and occludin have been seen in chronic sleep deprived individuals, who also demonstrated increased intravenous contrast extravasation from the BBB on neuroimaging [47]. Recent evidence from animal models has also demonstrated that the claudin-5 gene (CLDN5) is regulated by the transcription factor BMAL1 and the circadian clock [43]. Claudin-5 expression was demonstrated to be lower in the evening compared to the morning in mice throughout various tissues sampled [43]. An unhealthy diet rich in fats and sugars is a risk factor for AMD development [32]. In the same study, depigmentation and atrophy of the RPE, a classic feature of AMD, was present in claudin-5 suppressed mice fed a cholesterol rich diet [43]. As claudin -5 is not expressed in the RPE, the authors concluded that a diffusion of molecules from the iBRB must have a deleterious effect on the RPE.

Optical coherence tomography (OCT) is a useful tool for the assessment of RPE integrity, macular thickness, and can detect intra and subretinal fluid. Fundus fluorescein angiography (FFA) allows visualisation of blood vessels of both the choroidal and retina, therefore allowing identification of CNV or areas of RPE atrophy [33]. Fluorescein can pass freely through the fenestrated choriocapillaries, but in the healthy retina, endothelial cells of the iBRB do not allow clinical fluorescein extravasation [33].

However, the Campbell lab (Dr. Jeffrey O’Callaghan) has developed novel Fluorescent Ocular Vascular Analysis Software (FOVAS) which can detect sub clinical fluorescein present in the retinal parenchyma at the macula. This is measured as a proxy for iBRB permeability. Quantification of a “normal” fluorescein signal at the macula is now possible and an experimental participant can now be compared to this “normal group” and any changes in fluorescein signal (i.e., whether it is increased or decreased relative to the “normal”) can be seen.

Previous research has demonstrated a circadian difference in fluorescein diffusion concentration in the retinas of young healthy human controls and non-human primates. Increased fluorescein diffusion is seen in the evening compared to the morning FFA’s when

measured using FOVAS [43]. This increased iBRB permeability in the evening relative to the morning is thought to be the normal cycle of events in the healthy state. This finding correlates well with decreased claudin-5 expression in the evening in the animal studies reported above, thereby suggesting a decreased TJ barrier in the evening [43].

1.4 The blood brain barrier (BBB) and BRB similarities

The brain, like the retina, is also a highly privileged site and contains a neurovascular barrier, the blood brain barrier (BBB). The BBB describes the separation of the neural tissue from the systemic circulation by the endothelial cells and their TJs of the cerebral vessels [48]. The BBB has a very similar composition and function as the iBRB, as its main components consist of a NVU, endothelial cells of blood vessels, and TJ components which all regulate the flow of material to neural tissue like in the retina [48, 49].

Endothelial cells of the BBB, like in the BRB, have reduced rates of transcytosis, higher expression of claudins, occludins and other TJ proteins compared to other areas of the body and thus prevent the diffusion of molecules greater than 400kDa [26]. BBB disruption has been increasingly reported in several neurological conditions including acute events (stroke, concussion) and chronic events including chronic traumatic encephalopathy (CTE), Alzheimer's disease and Parkinson's disease [92]. BBB breakdown also leads to extravascular leakage, reduced TJ expression, increased transcellular transport and inflammatory cell infiltration, processes also seen in BRB breakdown and retinal disease [48].

Neuronal cells in both tissues also contain similarities. Retinal ganglion cells have features near identical to neurons in the brain, namely dendrites, a cell body and an axon, which join to form the optic nerve [49]. The main glial cell in the brain is the astrocyte. Whilst the retina does contain astrocytes, it is the Müller cell in the retina which is the dominant glial cell fulfilling similar functions to the astrocyte in the brain [50]. These cells are in contact with blood vessels and neurons and thus can influence neuron transmission through regulation of neurotransmitter levels, and control tissue blood flow via influences on vasoconstriction and vasodilation [50].

New evidence is emerging that the retina may act as a biomarker for disease in the brain involving BBB dysfunction and vice-versa [49,51]. Thus, by understanding the underlying dysfunction of the disease process in the brain, and particularly in conditions with underlying BBB dysfunction, retinal and iBRB analysis may be an early, non-invasive, inexpensive, and accessible way of investigating neurological diseases [49,51].

Studies have shown an association between changes in the retina and the brain in microvascular diseases such as diabetes and hypertension. The degree of haemorrhages and lipid exudation in the retina correlated with white matter changes visualised on MRI brain [51]. Similarly, dysfunction of the NVU typically occurs earlier in the retina compared to the brain, clinically manifesting as diabetic retinopathy, which can be directly visualised [52].

Other aspects also make the eye suitable for the study of CNS disease. Firstly, it is reasonably accessible making imaging easier, quicker and better tolerated than neuroimaging [49]. Secondly, as the retinal layers and blood vessels can be easily visualised, any disruption for example in the retinal ganglion cell or blood vessels can be seen, quantified, and localised [49]. As neuronal cell loss and BBB leakage are common in many neurological conditions, retinal imaging could act as a surrogate for measurement of the same dysfunction taking place in the

brain and thus avoid the need for more invasive, time consuming and costly neuroimaging techniques [49,51].

This study therefore aims to clinically investigate one of these neurological conditions with known BBB dysfunction, Visual Snow Syndrome, using retinal examination and iBRB imaging techniques.

1.5 Visual Snow Syndrome

Visual snow (VS) is a relatively novel neurological condition defined by the constant presence of positive visual phenomenon in visual fields of both eyes [53]. Black, white, transparent, and coloured static have been described in addition to “floaters” and flashing light phenomenon [53, 54]. The condition is painless. Some authors have published a diagnostic criteria for VS syndrome which includes the presence of the above visual effects in addition to the presence of two of the following four visual symptoms: photophobia (severe sensitivity to light), palinopsia (the presence of an “afterimage” of an object that is now outside the visual field), entoptic phenomenon (visualisation of images/objects within the eye itself, not physically present in the external environment) and nyctalopia (poor night vision) [53, 54]. Ophthalmological pathology should also be excluded before a diagnosis of VS is given. Figure 2 shows a visual representation of VS.

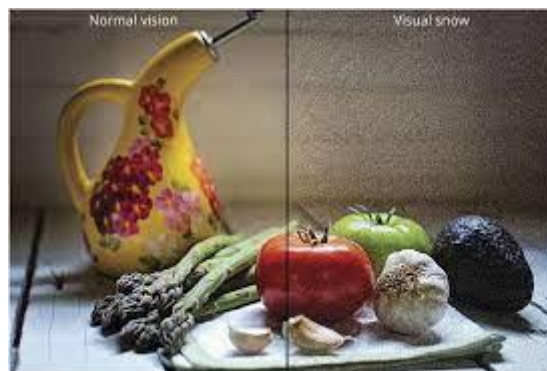


Figure 2: A representation of visual snow

Source: Puledda F, Schankin C, Goadsby PJ. Visual snow syndrome: a clinical and phenotypical description of 1,100 cases. *Neurology*. 2020 Feb 11;94(6): e564-74.

In addition, tinnitus and migraine are strongly associated with the condition, and is important to distinguish the intermittent visual aura seen in migraine with the constant visual “static” seen in VS [53, 54]. It is also important to rule out the use of recreational drugs in the one to two years preceding diagnosis as similar visual symptoms have been described in hallucinogen persisting perception disorder (HPPD), a condition which, as the name suggests, results in continued visual disturbance after the use of psychoactive substances [53, 54].

The mechanisms underlying visual snow remain poorly understood. One study examining metabolism in the brain using PET scans showed increased uptake and thus activity in the lingual gyrus, located in the supplementary visual cortex, involved with processing visual

inputs [55]. Interestingly, a further study using PET scans demonstrated excitability of the visual cortex in response to photophobia during a migraine attack [56]. These findings may explain abnormal excitability pathways present in both conditions and thus the association between migraine, VS and increasing intensity of VS symptoms during a migraine attack [57].

A recent study has demonstrated decreased amplitude and increased latency in visual evoked potentials in VS patients, suggesting some dysfunction of the visual association cortex [55, 58]. A retrospective study involving 28 patients demonstrated normal ophthalmological findings on review. In addition, different medications (lamotrigine, topiramate, propranolol) were trialled in this patient cohort with general poor compliance and no improvement in symptoms noticed [58].

1.6 Aims and Objectives

In the longitudinal AMD IRCP study, we will determine if a circadian derived iBRB permeability difference is present during the early pathophysiological changes in AMD. We will achieve this by continuing recruitment of healthy young controls, age matched controls and participants with clinical signs of early AMD only. We will achieve this by using retinal fundus photography, FFA and OCT in the morning and the evening in the same individual to assess retinal blood vessel integrity and quantify iBRB permeability using a new automated imaging stacking technique in FOVAS termed “features”.

In VS, there is a gap in knowledge in the literature regarding the pathogenesis and underlying mechanisms, as discussed above. We aim to investigate whether any ocular pathology is evident in three participants reporting visual snow symptoms. A full ocular assessment and imaging using OCT and FFA will be carried out. Analysis of any iBRB permeability dysfunction will also be carried out using FOVAS.

METHODOLOGY

2.1 The AMD Irish Retinal Circadian project

Background

Participants were contacted and a discussion surrounding the project took place. A patient information leaflet and consent form were then emailed to the participant to read, which were then subsequently signed on the day of testing. On the day of testing, a health questionnaire and FFA consent form were also completed by the participant. In this way, informed consent was obtained for each participant.

Participants were required to attend once in the morning at approximately 7.30am and once in the evening at approximately 7pm. These visits took place on separate days, with an interval of at least two days, to allow the full excretion of the intravenous contrast agent sodium fluorescein 20% (used for retinal imaging) from the body.

There was no strict timeframe required to attend for the second visit, however the second visit was typically within a week of the first visit for most participants. The effect of daylight, and thus that of the seasons, on the circadian clock is typically to “reset” it based on the number of hours of daylight in a 24-hour period. However, as participants had their AM and PM measurements typically within a short space of time to one another (i.e., days to weeks) the effect of season change of increasing or decreasing hours of daylight would not have a material effect on the results. In addition, even though recruitment and imaging were carried out throughout the year, it is the statistical comparison between an individual’s images in the morning and evening visits which is important. In the future a subgroup analysis of participant’s who had imaging in the summer versus those in the winter would be interesting to compare.

Munich Chronotype Questionnaire

The Munich chronotype questionnaire was used to assess participants’ chronotype. A chronotype can be defined as the sleep and wake times a person has which is based on their circadian rhythm [74]. This questionnaire calculates the midpoint between the start and end of sleep to estimate an individual’s chronotype [75]. This was then used in statistical analysis when applying circadian rhythm influence on fluorescein imaging findings.

Health Questionnaire

The health questionnaire was used to obtain information related to participants medical history and demographic data including height, weight, age etc. This information was then used in the statistical analysis. Medical information included medication use, allergy, ethnicity, smoking, family and personal history of eye conditions, and past medical and surgical history.

Testing procedure

Visual acuity (VA) for each participant was measured at the start of the consultation at both the morning and evening visits. An ocular occluder was used to test VA in each eye with and without pinhole. Therefore, the best corrected visual acuity (BCVA) was measured for each eye. The ETDRS chart (a logMAR chart) was used for testing at 4 metres. As previous participants BCVA was calculated using the Snellen chart, a Snellen equivalent was calculated from the LogMar vision recorded as per the chart in use for each participant.

The central corneal thickness (CCT) was measured using a pachymeter prior to the measurement of each participant's intraocular pressure (IOP). The Perkins handheld applanation tonometer was used to measure the IOP of both eyes on both visits. Although the Goldmann applanation tonometer (GAT) is considered the gold standard in measuring IOP, the Perkins applanation tonometer has achieved similar IOP measurements compared to GAT, and is accepted in clinical practice [76]. An eyedrop (fluorescein sodium 0.25% with proxymetacaine hydrochloride 0.5%) was introduced into each eye prior to CCT and IOP check. An IOP >25mmHg, taking account of adjustments for CCT, meant participants pupils were not dilated due to the risk of increasing IOP further. Participants were asked to reattend if this was the case. Tropicamide 1% was used to dilate the pupils. On the first visit both pupils were dilated so as fundus photographs of both eyes could be taken for the severity grading of AMD. On the second visit only one eye was dilated, the eye with a clinically more advanced stage of AMD based on the grading system and the one used for imaging on the first visit.

Blood samples were collected both in the morning and evening visits following peripheral venous insertion of a 22-gauge cannula. Three purple EDTA blood collection tubes were collected to analyse DNA AMD risk variants: apolipoprotein-E (APOE), complement factor H (CFH) polymorphism, Age-related maculopathy susceptibility 2 (ARMS2), complement factor B (CFB), complement 3 (C3) and complement factor inhibitor (CFI). A yellow serum tube was used to analyse melatonin and cortisol levels. One PAXgene red topped tube was used to isolate RNA levels of clock components: BMAL-1, Per-2 and REV-ERB α . These samples will be used for future studies including correlating results with fluorescein angiography imaging findings outlined below.

The retinal camera Topcon 50ex was used to take fundal images of both eyes during the first visit. These were colour images focusing on the macula region, which were then used to categorise AMD severity or confirm no clinical findings of AMD were present in the control groups as per the modified grading system previously discussed.

Optical Coherence Tomography and Fundus Autofluorescence Imaging Acquisition

One eye was then assigned as the eye to be used for optical coherence tomography and fundus fluorescein angiography. Eyes from the control group were chosen at random. Eyes from the AMD group, where the same grading of AMD was present in both eyes, were also chosen at random. For AMD participants who had different grading in each eye, the eye with the more severe grading was chosen. The Heidelberg Spectralis (*Heidelberg Engineering, Heidelberg, Germany*) was used to acquire images centred on the macula. A 72-line raster image technique

was used to acquire a “volume scan” allowing precise visualisation of the different retinal layers in that region.

Following this, FFA images were acquired over a ten-minute period. Images were taken initially over the first minute following the introduction of 2ml of sodium fluorescein 20% w/v (400mg) followed by 2ml of NaCl 0.9% into the 22-gauge cannula previously inserted. Images were then captured over 10 minutes, typically at 2-minute intervals. This technique allowed participants to periodically sit back and rest throughout the ten minutes, thus improving participant compliance and image quality when they returned to the chin rest. The OCT and FFA imaging were then repeated on the second visit.

The final step was the removal of the intravenous cannula, and the organisation of transport home for the participant, as their pupils were dilated so they could not drive. CCT, IOP and VA values were recorded in addition to times of dilatation and bloods taken.

AMD classification and grading

The colour fundal photographs taken of both eyes from participants during their first visit were used to grade the severity of AMD for each participant. When clinical signs of AMD were present in both eyes, the eye with the more severe form of AMD was used for grading. A modified version of the International Classification and Grading system for AMD was used [72]. Three categories of early AMD replaced the ARM category in this classification [73].

The following categories were defined:

Category 1: no disease (no age-related macular changes)

Category 2: early mild AMD (>10 hard drusen <63 μm)

Category 3: early moderate AMD (at least one soft druse >125 μm)

Category 4: early severe AMD (soft drusen and hyperpigmentation)

Category 5: late (choroidal neovascularisation)

Category 6: late (geographic atrophy)

Category 7: late (mixed CNV and GA)

Inclusion and exclusion criteria for AMD patients and age-matched controls:

Inclusion criteria for the AMD group: male or female with a diagnosis of early or moderate AMD graded 2,3 or, 4 as per the modified version of the International Classification and Grading System for AMD.

Inclusion criteria for the age-matched control group: male and female participants >65 years of age graded as 1 as per the classification system. Post operative patients who had undergone removal of cataract surgery and were attending for routine post operative visits.

Exclusion criteria for both groups: A significant ocular diagnosis such as recent ocular surgery within three months, retinal vascular occlusion, retinal detachment, diabetic retinopathy, or glaucoma.

Recruitment numbers

Updated numbers for statistical analysis using “features” based analysis across all three recruitment groups are as follows: Young healthy control group (n=31). Age matched control group (n=13). AMD group (n=33). As this research is part of a longitudinal study titled the “Irish Retinal Circadian Project” numbers will continue to be added to each group over the coming months and years.



Figure 4. The Irish Retinal Circadian Project (IRCP) logo

2.2 Fluorescent Ocular Analysis Software

Dr. Jeffrey O’Callaghan has developed the Fluorescent Ocular Analysis Software (FOVAS), the key program which enables quantification and analysis of the fluorescein signal from a participant’s FFA. The fluorescein signal is quantified in each area of the ETDRS grid- namely the fovea, parafovea, extrafovea and the overall signal from the macula area.

iBRB integrity can be assessed using this software. Clinically, areas of hyperfluorescence or hypofluorescence can be used to help diagnose disease. However, an amount of sodium fluorescein naturally leaves the inner retinal blood vessels, and this “subclinical level” fluorescence can be captured and analysed. The software was designed to be used with the Heidelberg Spectralis system used during the study. The macula area can be selected as the region of interest to be analysed and the ETDRS grid area specified and placed over this region for each participant thus allowing standardisation.

FOVAS is still unpublished work, with no other literature of equivalent software published to the best of our knowledge. However, FOVAS has been internally validated through other published work, with similar findings and intensity values in the experimental groups compared to the experimental groups in this study [43].

The delivery of sodium fluorescein from a peripheral blood vessel to the inner retinal vasculature leads to “brightness” or “hyperfluorescence” of the retinal vessels and retinal

parenchyma at the macula. The software measures the level of fluorescence in each area of the ETDRS grid from FFA images captured. It does this by measuring pixel intensity of the FFA image at the macula. The output is quantified on the y axis of the graphs below (in the results section) known as the “intensity value.” The brighter or more hyperfluorescent an area captured, the higher the pixel intensity, the larger an intensity value assigned, and the greater the value on the y axis. The “mean intensity values” from each participant in each of the three experimental groups can be pooled to give the mean intensity value of fluorescein signal for the entire group.

Statistical Tests

The raw data is first analysed to classify it as following a “normal” or “non-normal” distribution using the Anderson-Darling test. If the data follows a normal distribution, paired t-tests are used to compare paired data (e.g., intensity values from the same individual AM vs PM) or unpaired t-tests when data is compared across the different experimental groups (e.g., intensity values of the healthy control group vs the VS group).

If the data follows a non-normal distribution, then nonparametric tests are used. Wilcoxon signed rank test for paired comparisons and Wilcoxon rank sum test for unpaired comparisons. Most data to date has followed the non-normal distribution. P values for significance were calculated as per the above statistical tests and are represented in the results figures by *

Outlier data

The FOVAS data is presented in the results figures using the interquartile range (IQR). Each box within the dashed lines represents the middle 50% (IQR) of recorded values (i.e., 25%-75%). The dashed lines above and below the box represent the other quartiles. (i.e., 0-25% below the box and 75%-100% above the box). Each of these quartiles is calculated by: 1.5 times the IQR ($1.5 \times \text{IQR}$). Horizontal lines in each box represent the mean intensity values. Outliers are represented by red plus signs.

Of note, outliers were not excluded from statistical analysis and are included in the results. They are also included in the results figures below for illustration. Outliers were defined as values that are outside $1.5 \times \text{IQR}$. True exclusions from the data for statistical analysis included individual FFA images from different timepoints. These were manually removed from the “stacking” process described below if poor image quality was present due to patient or researcher factors. For example, blurring, dark images, blinking or delayed image capture.

FFA images or frames captured at different time points are aligned or “stacked”. The new “features” or automated analysis technique uses anatomical landmarks in the fundus such as the optic nerve head and retinal veins to standardise the analysis of fluorescein signal in the ETDRS zones of the macula. For example, all the images from a participant taken at AM and PM over the 10-minute imaging interval are overlaid or “stacked” using these landmarks and fluorescein intensity level is measured and differences recorded. In addition, as some poor-quality images are inevitably captured for each participant due to factors such as eye movement and blinking, manual exclusion of these images was performed as this can skew the analysis results.

This new technique has reduced time of manual review and manual overlay of each image captured, thus improving efficiency, and reducing operator error. Therefore, this new method built into the software is believed to be more accurate in its analysis. Therefore, analysis using this new technique was carried out for the experimental groups of the IRCP study and VS participants, now with a larger sample size, thus improving accuracy of interpretation of results further.

The software also allows comparison between “cumulative” AM and PM fluorescein signal from the same participant, comparison of AM and PM signal at each timepoint of FFA (e.g., 0.5-2mins, 2-6 mins, and 6-10mins) and comparison of signal between the healthy young control group and the other experimental groups (i.e., age matched control and AMD).



Figure 3. Example of ETDRS grid placed over macula. Fluorescein signal can then be quantified overall and within each ETDRS region

2.3 Visual Snow Syndrome

An open group twitter page through TCD was used to recruit patients with visual snow symptoms. Most clinicians are unfamiliar with VS, and as many people with VS have sought help from clinicians with little benefit, many used social media to connect with others who are experiencing similar symptoms and communities have grown online.

Participants were asked about specific symptoms to diagnose Visual Snow Syndrome, which consists of the “visual snow” in addition to having two of the following four symptoms: palinopsia (trailing of moving objects or afterimages), entoptic phenomena (visual experiences coming from within the eye), photophobia (sensitivity to light), and nyctalopia (poor vision in dim/dark light).

The VS study protocol was similar to the IRCP study protocol apart from FFA imaging. FFA images were acquired over a ten-minute period captured at approximately two-minute intervals at 2mins, 4mins, 6 mins, 8 mins and 10 mins as previous, however, images of both eyes were

taken at each imaging interval in contrast to images taken of one eye only in the IRCP study protocol.

RESULTS

3.1 The AMD Irish Retinal Circadian project

3.1.1 Participant sample images

Figures 3 and 4 below gives sample fundal images taken from participants recruited this year and their corresponding AMD grade of disease as per figure in the methods section.

Grade 1 participants are age matched controls and have no clinical signs of AMD at the macula. Grade 2 participants have greater than ten “hard” drusen measuring $<62\mu\text{m}$. Grade 3 participants have at least one “soft” drusen measuring $>125\mu\text{m}$. Grade 4 participants have “early severe” disease characterised by soft drusen and hyperpigmentation. Grades 5, 6 and 7 represent advanced disease and are not included in the study.

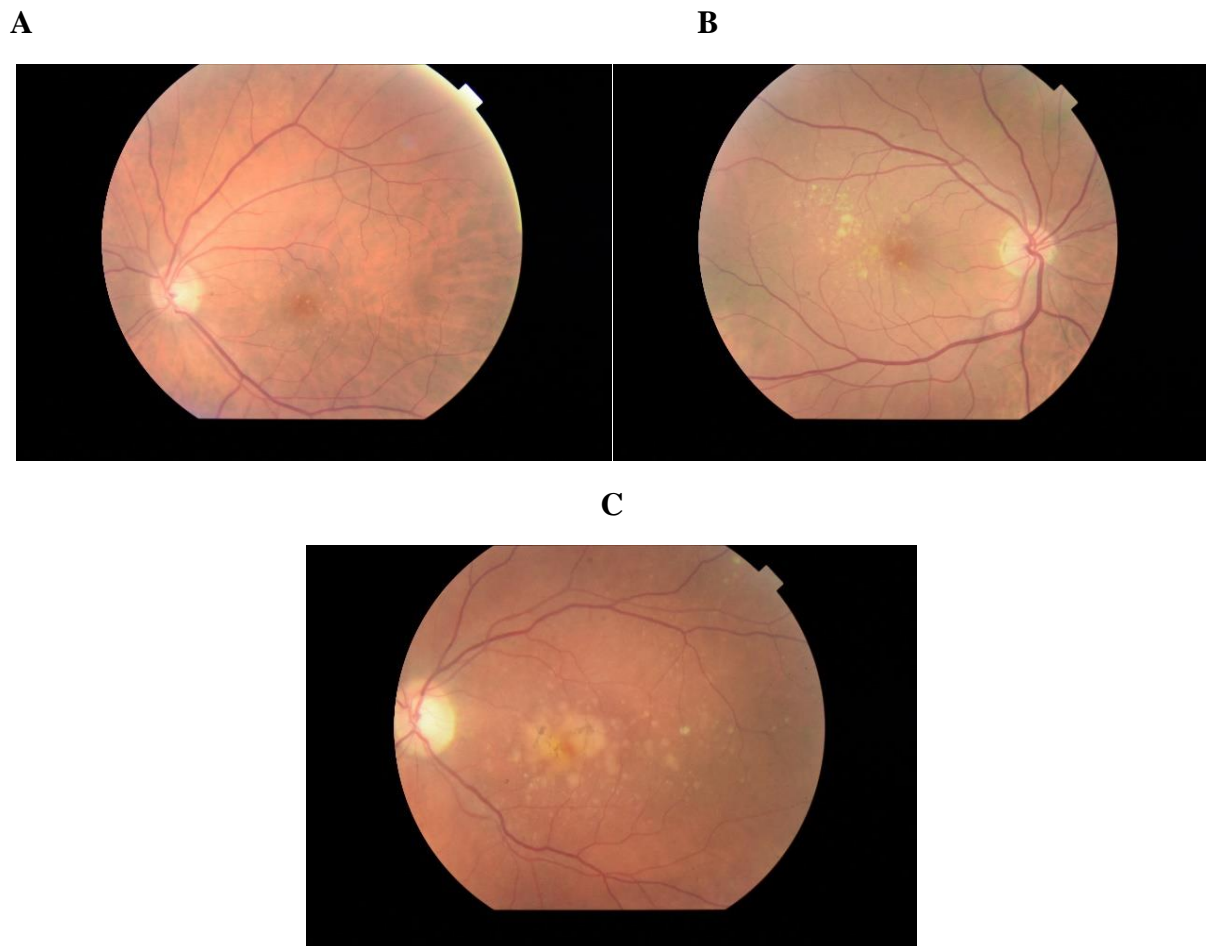
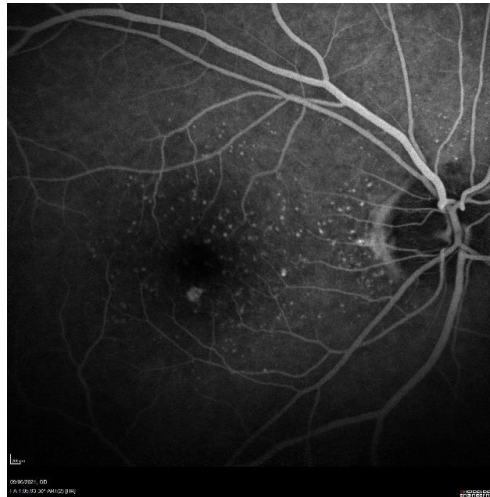
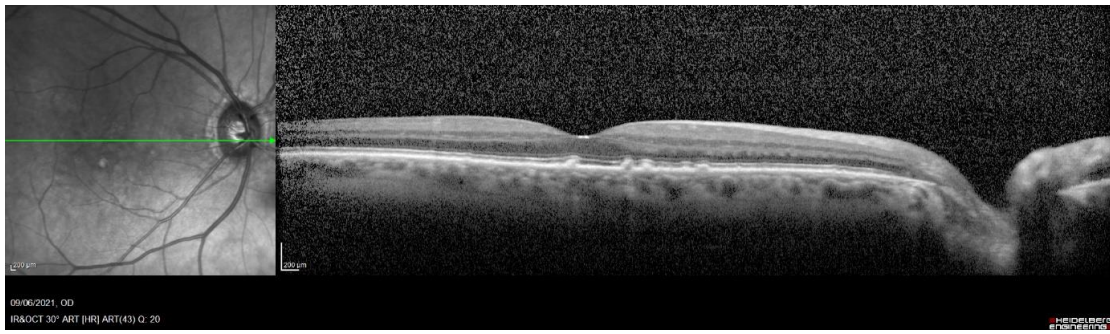
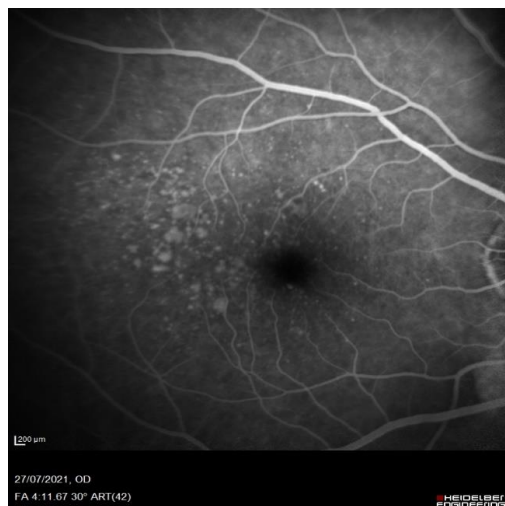
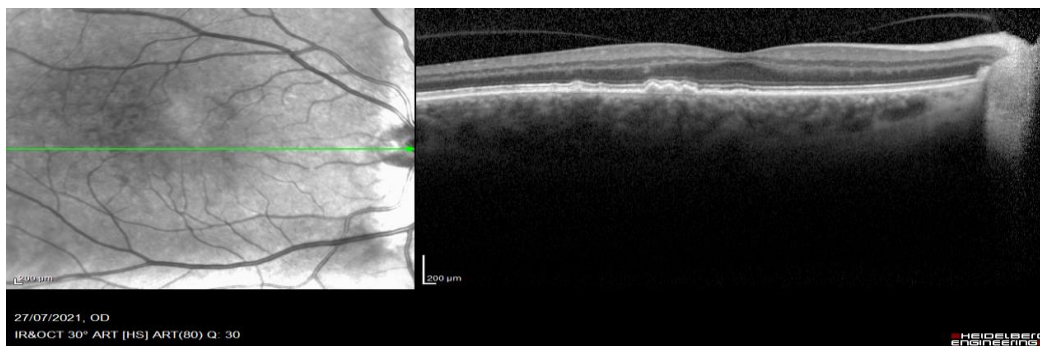


Figure 3: Macular fundus photos from participants demonstrating the clinical grades of disease in AMD that were recruited to the study. A. Grade 2 B. Grade 3 C. Grade 4

A



B



C

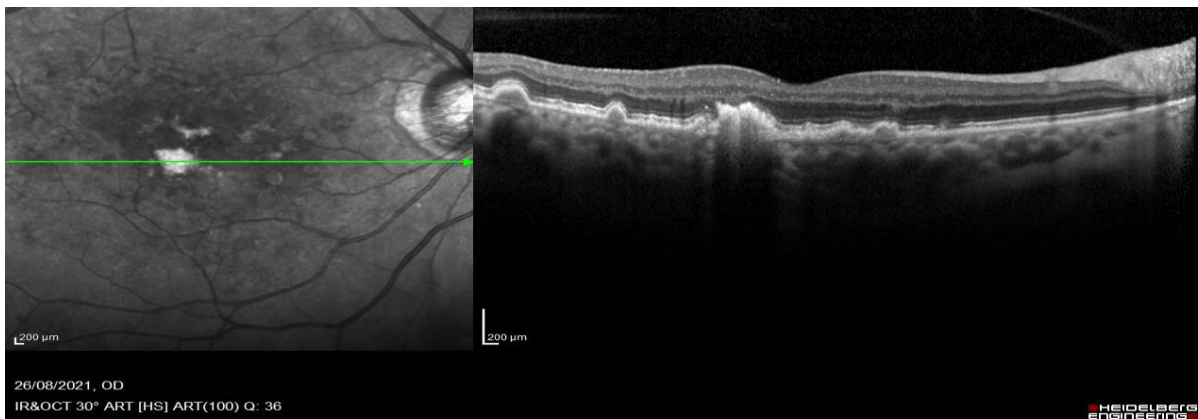


**Figure 4: Macular OCT and FFA images taken from the same participants as the fundal photos above demonstrating the clinical grades of disease in AMD in the study.
A. Grade 2 B. Grade 3 C. Grade 4.**

Figure 5 below demonstrates FFA images from participants captured at timepoints over 10 mins in both young healthy controls and AMD. Images below demonstrate early (0.5-2 mins), mid (2-6 mins) and late (6-10 mins) phase in both the AM and PM imaging session. The ETDRS grid can then be placed over these images and the fluorescein signal quantified as per FOVAS. Note in the top image below of the healthy young participant that the fluorescein signal at the macula appears “brighter” in the PM images compared to the AM images. In contrast, the bottom image represents FFA images from an AMD participant. Ignoring the peripheral darkness (artefact from the lens camera), note how the fluorescein signal at the macula appears similar intensity or “brightness” in both the PM and AM images.

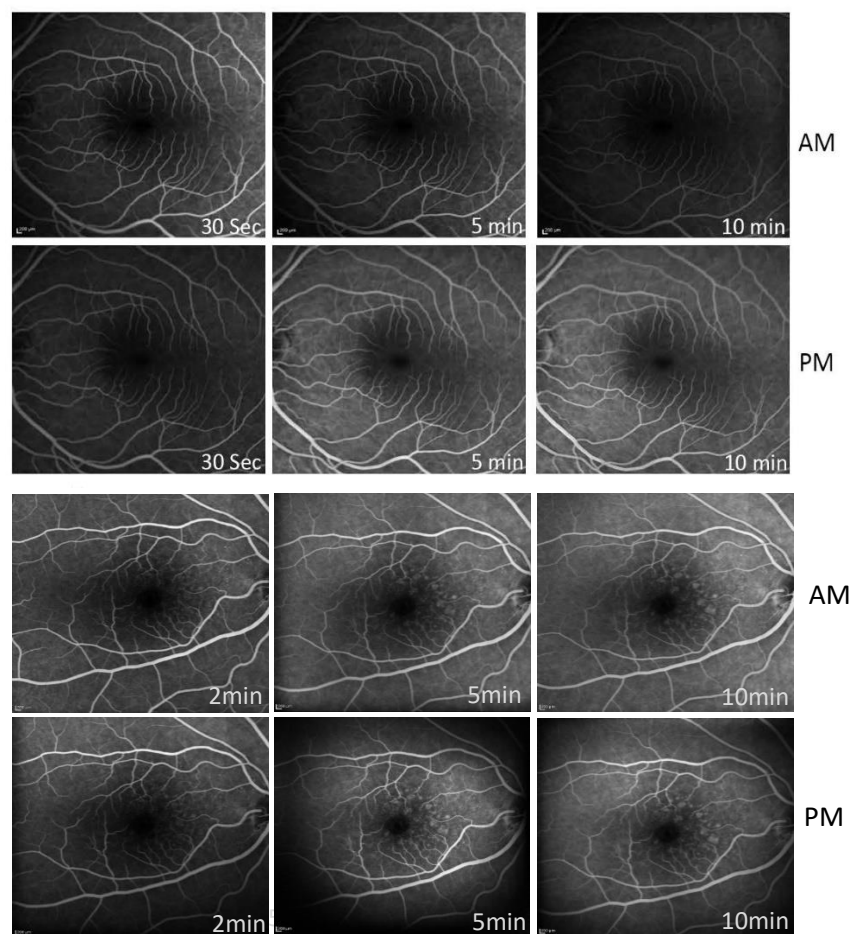


Figure 5: Top image: FFA images of a healthy young control participant captured over 10 mins in both the AM and PM imaging session.

Bottom image: FFA images of a participant with AMD captured over the same timeframe in both AM and PM.

3.1.2 In the healthy young control group (n=31) a higher mean fluorescein signal is seen in the evening compared to the morning in all ETDRS areas of the macula and throughout all timepoints of the FFA, some of which is statistically significant

Automated analysis using the FOVAS software of FFA images from healthy young participants was performed. The total number of participants analysed in the healthy control group, aged 18 to 30 years, is now 31. FFA images were taken over 10 minutes during early (0.5-2minutes), mid (2-6 minutes) and late (6-10 minutes) phase intervals. Each participant attended twice-once in the morning (AM) and once in the evening (PM). The y axis represents the mean intensity value of fluorescein signal. The x axis represents each ETDRS area of the macula analysed, from the fovea to the extrafovea and overall.

Figure 6 shows the measured cumulative mean intensity value of fluorescein signal measured for AM (blue boxes) and PM (red boxes) throughout all ETDRS areas of the macula in this group. The results figures are presented using the interquartile range (IQR) method as outlined in the Methods (section 2.2) above. The cumulative mean intensity level is higher in the PM compared to the AM throughout all areas of the macula in the healthy young control group. At the fovea, the cumulative mean intensity level is significantly higher in the PM vs AM (*P=0.04).

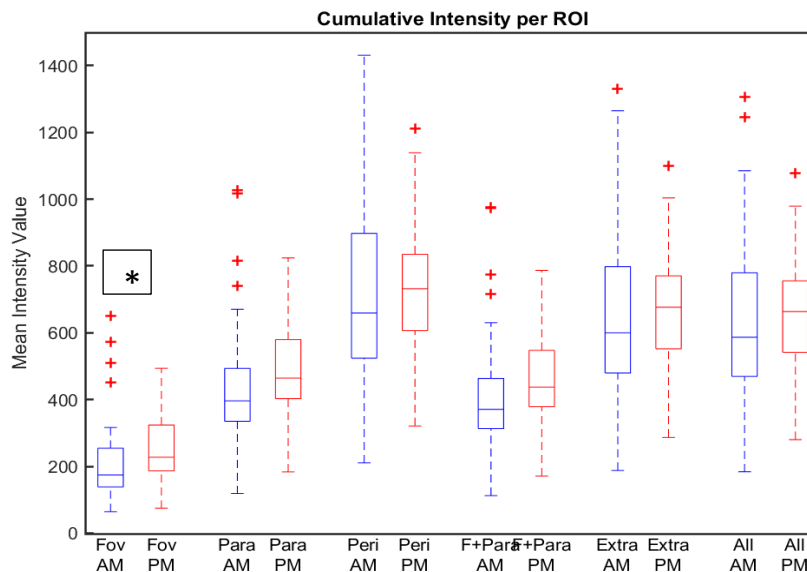


Figure 6: The measured cumulative mean intensity for AM and PM throughout all ETDRS areas of the macula for the young healthy control group (n=31). The mean intensity level is higher in the PM compared to the AM throughout all areas of the macula. At the fovea, the cumulative mean intensity level is significantly higher in the PM vs AM (*P=0.04)

Next, the percentage difference of mean intensity value between the PM and AM in the healthy young control group was calculated using automated FOVAS analysis. In figure 7, the range of intensity values is again represented between the dashed lines and 75% within the blue box, with outliers represented by red plus signs. The y axis now represents the percentage difference of mean intensity values between the PM and AM. The AM mean intensity value is represented by the horizontal line running across the graph at 0%. The PM mean intensity value is represented by the red horizontal line within each blue box. This AM mean intensity value therefore acts as the “baseline at 0%” and the PM mean intensity value measured can be compared to this.

For example, at the fovea we can see that the PM mean intensity value is located between 0 and 50% (it is 22%). Therefore, we can conclude that in the young healthy control group, at the fovea, there is a 22% increase in mean intensity value of fluorescein signal during the PM compared to the AM, indicating more fluorescein has leaked out of the iBRB in the PM compared to the AM, and this is statistically significant (*P=0.004). Significantly increased also at the parafovea (*P=0.01), and fovea+parafovea (*P=0.01).

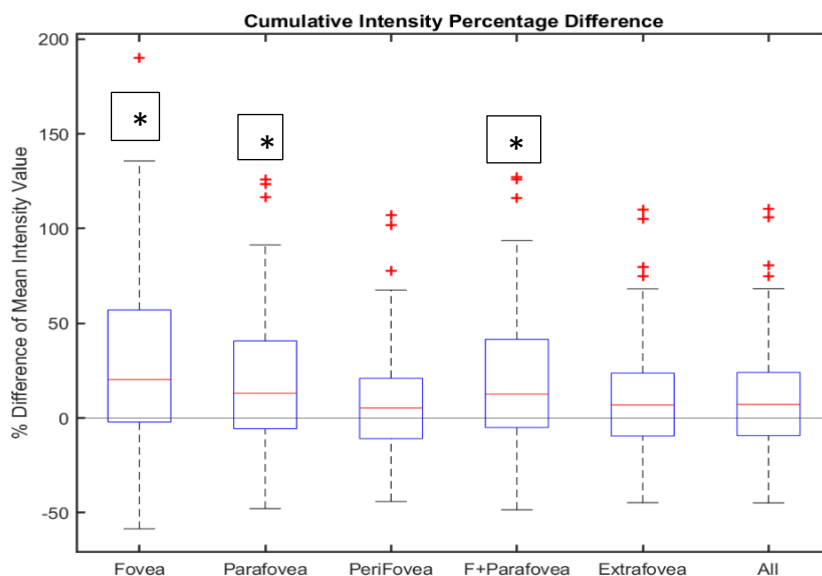


Figure 7: The mean intensity value percentage difference between AM and PM. All regions of the macula demonstrate an increase in the mean intensity value fluorescein signal in the PM compared to the AM represented by all PM lines above the continuous 0% AM line. Significantly increased at the fovea(*P=0.004), parafovea (*P=0.01), and fovea+parafovea (*P=0.01).

Next, the percentage difference of mean intensity value between the PM and AM during different timepoints of the FFA in the healthy young control group was calculated using automated FOVAS analysis to see if the increased PM vs AM signal observed occurred at any timepoint during the FFA. The mean intensity percentage difference between the AM and PM during early (0.5-2mins), mid (2-6mins) and late (6-10 mins) phases during imaging was

analysed (Figure 8). All regions of the macula demonstrate an increase in the mean fluorescein signal in the PM compared to the AM in all phases. This is significantly increased at mid phase in all areas of the macula (*P<0.05) and in the late phase at the fovea (*P=0.04).

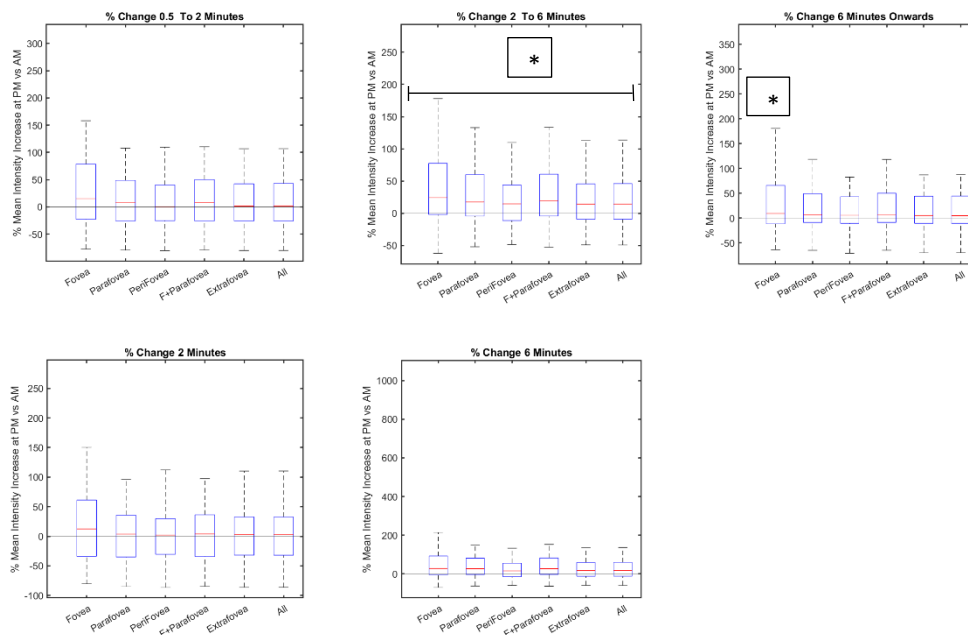


Figure 8: The mean intensity percentage difference between AM and PM during early (0.5-2mins), mid (2-6mins) and late (6-10 mins) phases of FFA in the healthy young control group. All regions of the macula demonstrate an increase in the mean fluorescein signal in the PM compared to the AM in all phases. Significantly increased at mid phase in all areas of the macula (*P<0.05) and in the late phase at the fovea (*P=0.04)

3.1.3 In the age-matched control group (n=13) a higher mean fluorescein signal is seen in the evening compared to the morning in all ETDRS areas of the macula (except the fovea). However, there is a smaller difference compared to the healthy young control group and is not statistically significant

Automated analysis using the FOVAS software of FFA images from age matched control participants was performed. The total number of participants analysed in the age matched control group, aged greater than 65 years, is now 13. FFA images were taken over 10 minutes during early (0.5-2minutes), mid (2-6 minutes) and late (6-10 minutes) phase intervals. Figure 9 shows the measured cumulative mean intensity value for AM (blue boxes) and PM (red boxes) throughout all ETDRS areas of the macula in this group. Some ETDRS regions show an increased mean intensity fluorescein signal in the PM compared to the AM (parafovea, perifovea, fovea and parafovea). However, this was not a statistically significant increase. Other areas (fovea and extrafovea) show similar mean intensity values in the PM and AM.

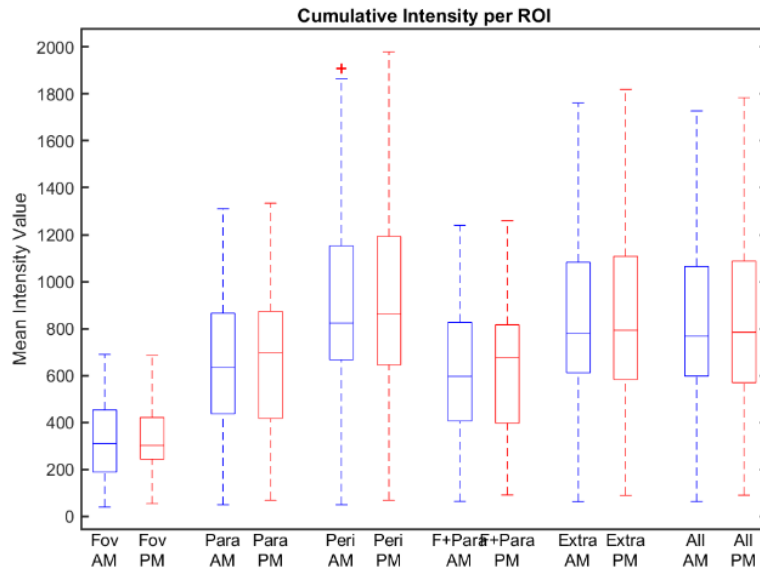


Figure 9: The measured cumulative mean intensity for AM and PM throughout all ETDRS areas of the macula for the age matched control group (n=13). The cumulative mean intensity values are not significantly increased in the PM vs AM in any ETDRS areas. Not significant (NS) for all.

Next, the percentage difference of mean intensity value between the PM and AM in the age matched control group was calculated using automated FOVAS analysis (Figure 10). Again, the AM mean intensity value is represented by the horizontal line running across the graph at 0%. The PM mean intensity value is represented by the red horizontal line within each blue box. There is an increased mean signal intensity percentage difference in the PM compared to the AM at all ETDRS areas of the macula (except for the fovea). However, this increase is not statistically significant.

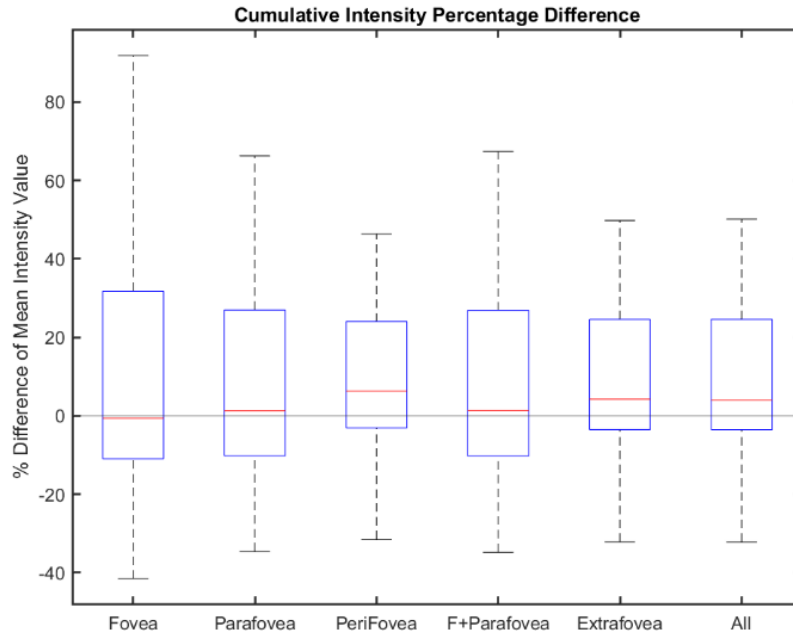


Figure 10: The mean intensity signal percentage difference between AM and PM in the age matched control group. All regions of the macula demonstrate an increase in the mean fluorescein signal in the PM compared to the AM (except for the fovea). Not significantly (NS) increased for all areas.

3.1.4 In the AMD group (n=13) no statistically significant difference is seen in the mean fluorescein signal in the evening compared to the morning in all ETDRS areas of the macula. There is also variability in the difference in mean fluorescein signal between the PM and AM signal throughout the different timepoints of the FFA.

Automated analysis using the FOVAS software of FFA images from early-stage AMD participants was performed. The total number of participants analysed in the AMD group is now 33. FFA images were taken over 10 minutes, during early (0.5-2minutes), mid (2-6 minutes) and late (6-10 minutes) phase intervals. Figure 11 shows the measured cumulative mean intensity value for AM (blue boxes) and PM (red boxes) throughout all ETDRS areas of the macula in this group. All ETDRS regions of the macula appear to show a slightly increased cumulative mean intensity signal in the PM, however this was not a statistically significant increase.

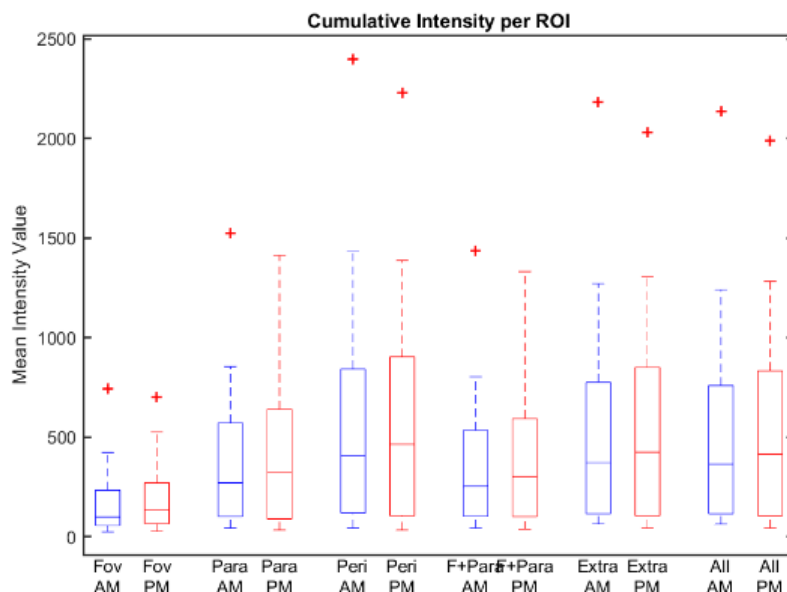


Figure 11: The measured cumulative mean intensity for AM and PM throughout all ETDRS areas of the macula for the early-stage AMD group (n=33). The cumulative mean intensity values are not significantly increased in the PM vs AM in any ETDRS areas. Not significant (NS) for all.

The percentage difference of mean intensity value between the PM and AM in the AMD group was again calculated using automated FOVAS analysis (Figure 12). Note that there is no mean signal intensity percentage difference in the PM compared to the AM in all ETDRS areas of the macula. Note how each PM mean intensity signal (the red horizontal line within each blue box) is indistinguishable from the AM mean intensity signal (the horizontal line running across the graph at 0%), indicating that the mean signal intensity in the AMD group is the same or very similar at both AM and PM imaging times.

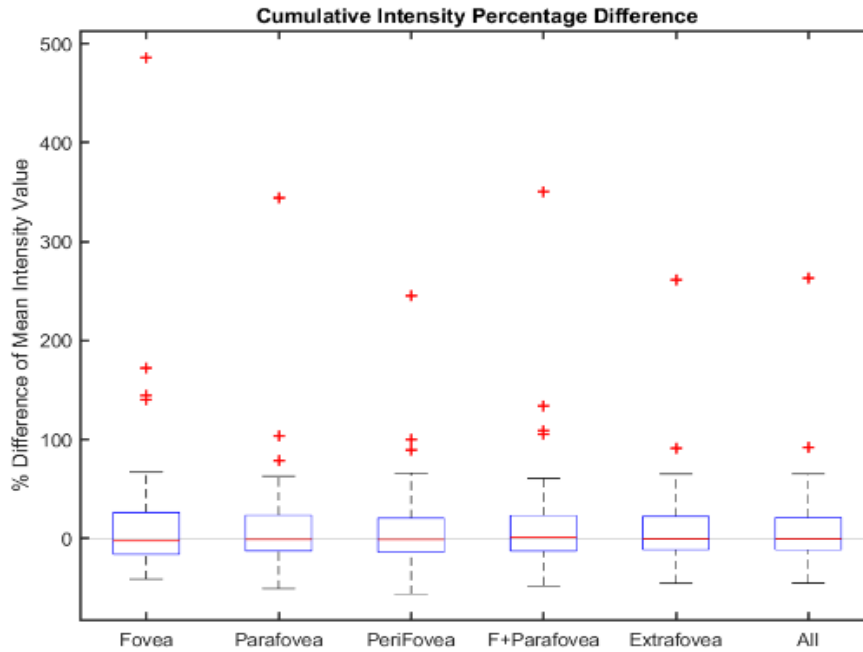


Figure 12: The mean intensity signal percentage difference between AM and PM in the early-stage AMD group. There is no percentage difference in the mean intensity value between the PM and AM throughout all ETDRS regions of the macula. Not significantly (NS) increased for all areas.

The percentage difference of mean intensity value between the PM and AM during different timepoints of the FFA in the early-stage AMD group was calculated using automated FOVAS analysis (Figure 13). The mean intensity percentage difference between the AM and PM during initial bolus (0-0.5 mins), early (0.5-2mins), mid (2-6mins) and late (6-10 mins) phases was analysed. All ETDRS regions of the macula demonstrate an increase in the mean fluorescein signal in the PM compared to the AM in the initial bolus, mid and late phases, however this was not significant. A significantly increased PM signal vs AM signal was seen at 6 minutes. A reversal was seen during the mid-phase, where a higher mean intensity fluorescein signal is seen in the AM compared to the PM. This contrasts with the healthy young control group, whereby a significantly higher mean intensity signal was seen in the PM compared to the AM during the mid-phase and late phase (at the fovea) and no significant differences seen during the other phases.

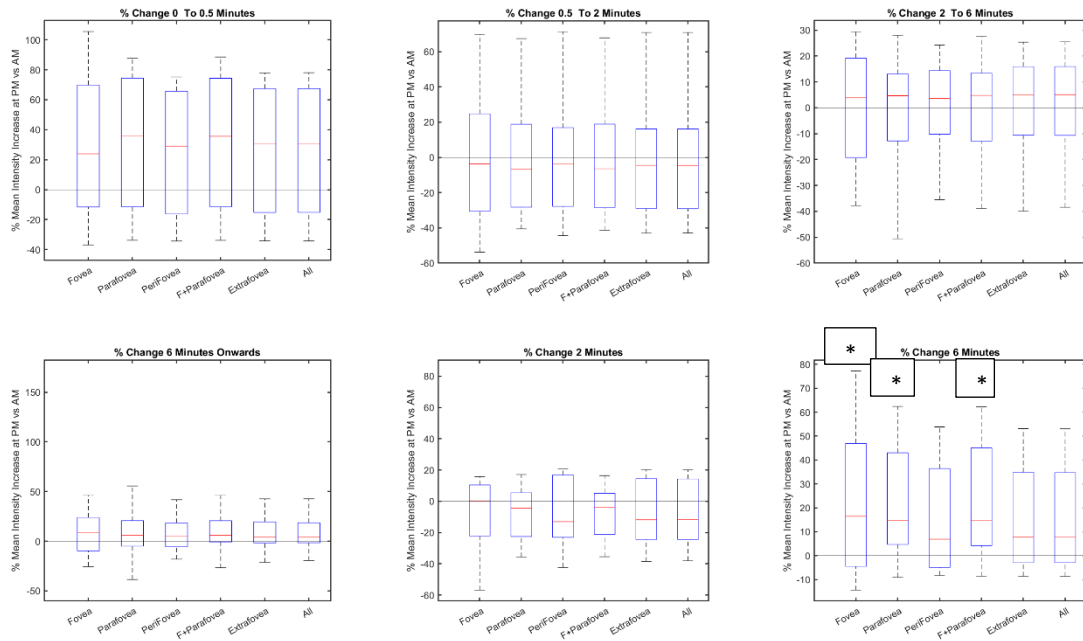


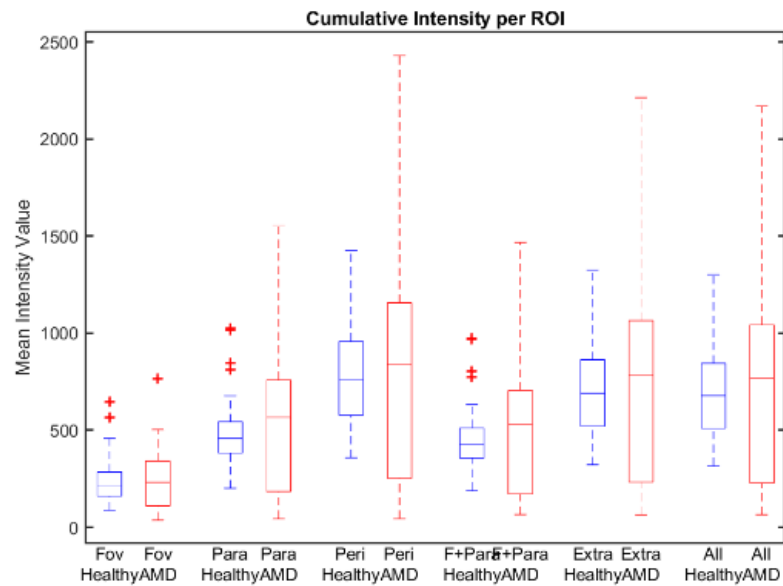
Figure 13: The mean intensity percentage difference between AM and PM during initial bolus (0-0.5 mins), early (0.5-2 mins), mid (2-6 mins) and late (6-10 mins) phases of FFA in the early-stage AMD group. All ETDRS regions of the macula demonstrate an increase in the mean fluorescein signal in the PM compared to the AM in the initial bolus, mid and late phases, however this was not significant. Statistically significant increased PM signal at 6 minutes. A reversal is seen during the early phase, where a higher mean intensity fluorescein signal is seen in the AM compared to the PM.

3.1.5 A higher mean cumulative fluorescein signal is seen in the PM in the healthy young control group compared to the AMD group. In contrast, this reverses in the AM, with a higher signal in the AMD group compared to the healthy young control group

Figure 14 shows and compares the measured cumulative mean intensity fluorescein signal for the healthy young control group (blue boxes) and the early-stage AMD group (red boxes) throughout all ETDRS areas of the macula at the AM imaging session and the PM imaging session. This is a useful comparator, as to date only intragroup data has been presented and compared.

In the AM, mean cumulative intensity values were higher in the AMD group compared to the healthy young control group. In the PM, mean cumulative intensity values were higher in the healthy young control group compared to the AMD group. This shows that there is a difference in cumulative mean intensity values between the two groups in all ETDRS areas in both the morning and evening.

AM



PM

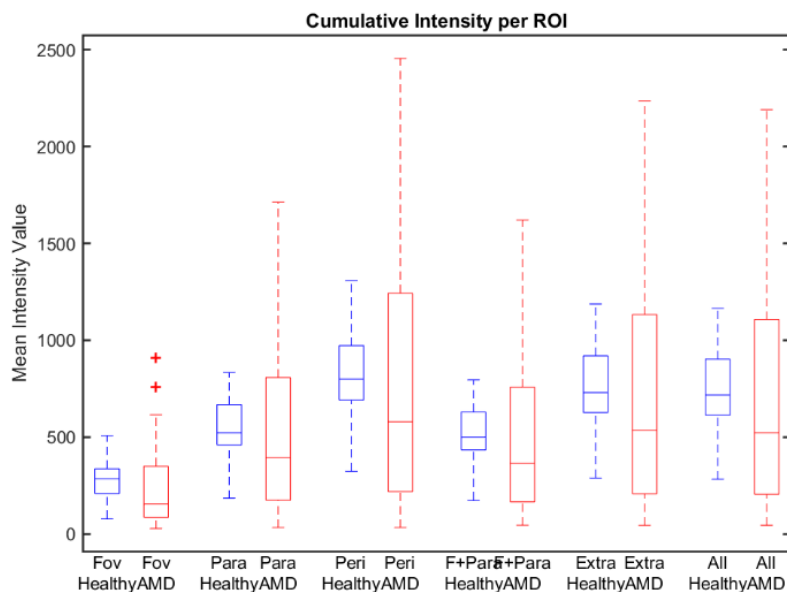


Figure 14 shows and compares the measured cumulative mean intensity fluorescein signal for the healthy young control group (blue boxes) and the early-stage AMD group (red boxes) throughout all ETDRS areas of the macula at the AM imaging session and the PM imaging session. In the AM, mean cumulative intensity values were higher in the AMD group compared to the healthy young control group. In the PM, mean cumulative intensity values were higher in the healthy young control group compared to the AMD group.

>> x axis: “Fov” (Fovea), “Para” (Parafovea), “Peri” (Perifovea), “F+Para” (Fovea +Parafovea), “Extra” (Extrafovea)

3.2 Visual Snow Syndrome

Three participants reporting visual snow symptoms were assessed. All participants reported constant black and white “static” present in both eyes, regardless of whether eyes were open or closed. Age of onset differed between participants but began in all in their late teens to early twenties. Entoptic phenomenon was reported by one, described as “electron blue” light present most notable with the eyes closed. Palinopsia, where the presence of an image remains for a few seconds in the visual field after the object is outside the field of view was also present in one participant. No obviously severe photophobia and nyctalopia were reported. Two participants reported long standing intermittent tinnitus and migraine symptoms, one was receiving active treatment for migraine. Interestingly, the frequency and intensity of visual static was reported to increase during the acute phase of a migraine, and a reduction in symptom intensity reported when the migraine began to abate.

Past ocular history in all revealed no previous ophthalmological conditions, trauma, infection, or surgery. No history of neurological disease was reported by any participants. No regular medication was taken by any of the participants apart from over-the-counter pain relief and prescribed oral medication for migraine attacks. No history of recreational drug use was reported, important for ruling out HPPD. There was no family history of VS symptoms reported, though two participants reported a family history of migraine in a first degree relative.

Relevant clinical data obtained during the consultations is included in Table 1 below. Each of the three participants were given a study ID. VS3, VS4 and VS5.

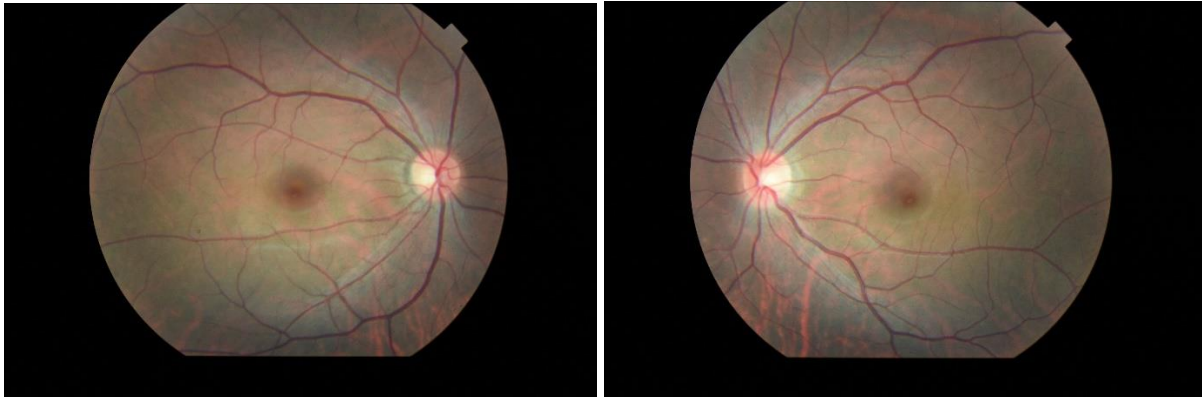
Table 1. Relevant clinical information from the three visual snow participants

	BCVA _{OD}	BCVA _{OS}	CCT _{μm} _{OD}	CCT _{μm} _{OS}	IOP _{OD}	IOP _{OS}
Control	6/6	6/6	562	555	11	13
VS3	6/7.5 ⁻¹	6/6 ⁻²	522	535	14	16
VS4	6/7.5	6/6	542	539	12	14
VS5	6/7.5 ⁻²	6/6	545	539	14	16

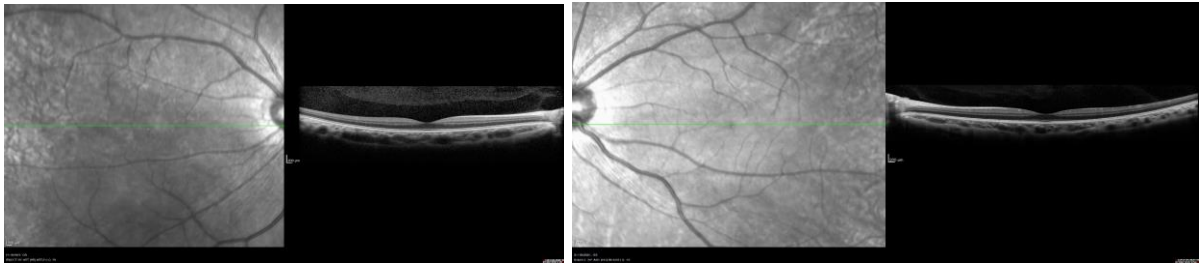
Bilateral Topcon Fundus photos were obtained. OCT and FFA were then performed over 10 mins as per the IRCP study protocol.

3.2.1 Participant images

(A)



(B)



(C)

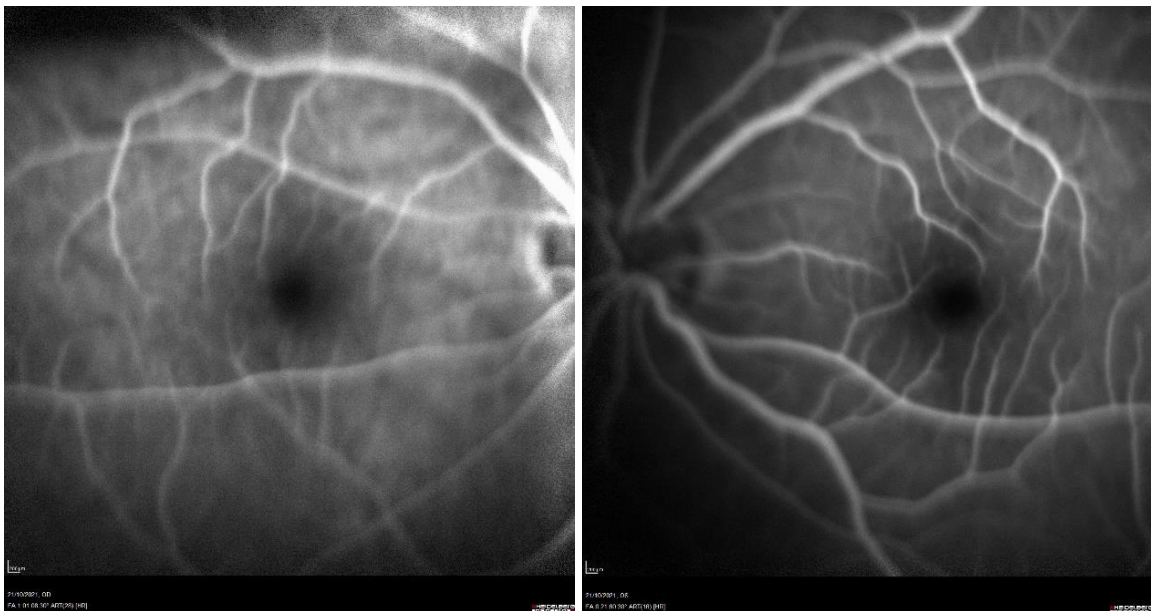
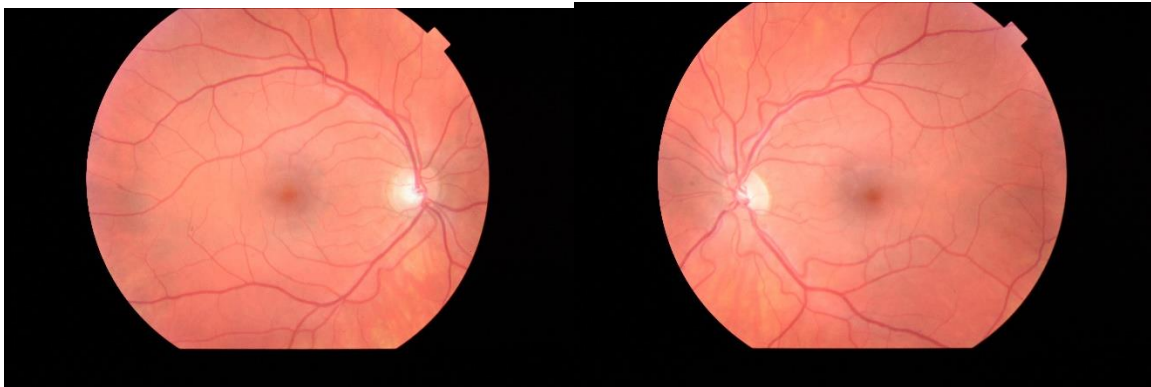
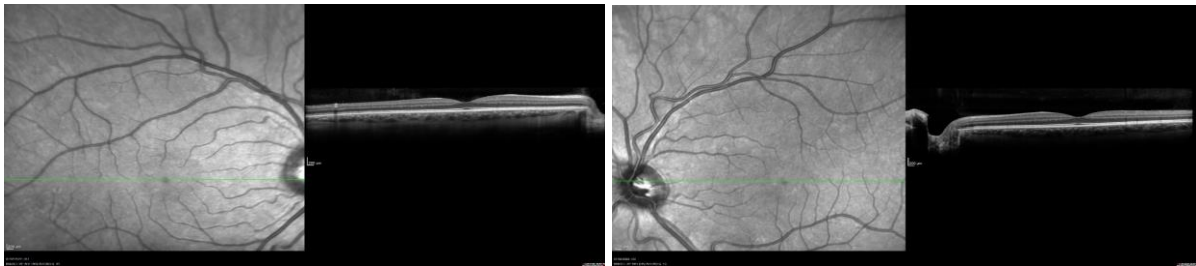


Figure 15: Fundus photos (A) Macular OCT (B) and FFA images (C) of the right and left eye from the VS3 participant. The right eye is the first image presented when reading left to right or top to bottom. Some inferior retinal lattice degeneration bilaterally is evident on fundal photos. No other clinical findings evident.

(A)



(B)



(C)

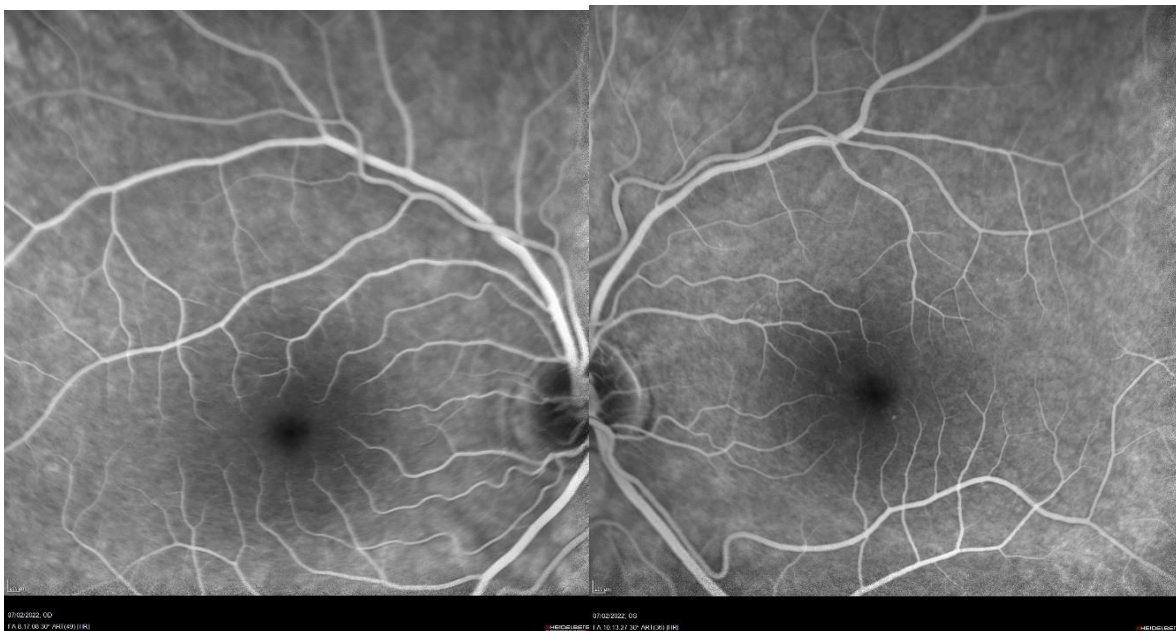
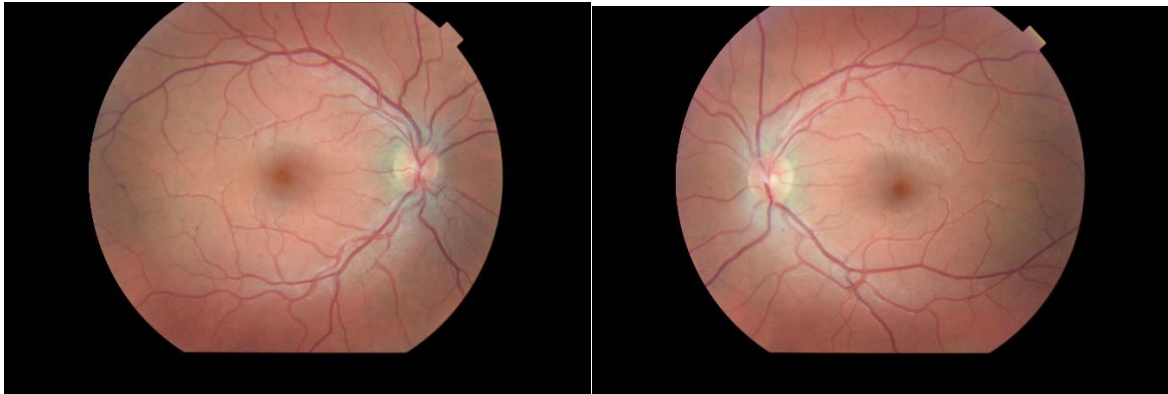


Figure 16: Fundus photos (A) Macular OCT (B) and FFA images (C) of the right and left eye from VS4 participant. The right eye is the first image presented when reading left to right or top to bottom. Grossly normal clinical findings.

(A)



(B)



(C)



Figure 17: Fundus photos (A) Macular OCT (B) and FFA images (C) of the right and left eye from VS5 participant. The right eye is the first image presented when reading left to right or top to bottom. Some silver wiring of retinal arterioles is evident bilaterally on fundal photos. No other clinical findings evident.

3.2.2 A higher cumulative mean intensity fluorescein signal was seen in individual and grouped analysis of the Visual Snow data (n=3) compared to the healthy young control group, most of which was statistically significant

Automated analysis using the new “features” based technique in FOVAS of FFA images from visual snow participants was performed. The total participant number is now five, including two others previously analysed (VS1 and VS2). The key result of interest was the measured cumulative mean intensity value for each VS participant compared to the cumulative mean intensity value of the healthy young control group from the IRCP study. As VS3 and VS5 were analysed in the evening time, the cumulative mean intensity value was compared to the PM cumulative mean intensity value from the healthy young control group as reported in the IRCP results section above. Similarly, as VS4 was analysed in the morning time, the cumulative mean intensity value of VS4 was compared to the AM cumulative mean intensity value from the healthy young control group. In addition, as visual snow symptoms are reported in both eyes, both eyes from each participant were analysed and results reported (e.g., separate analysis for VS3 right eye vs PM healthy young control results and VS3 left eye vs PM healthy young controls).

FFA images were taken over 10 minutes during early (0.5-2minutes), mid (2-6 minutes) and late (6-10 minutes) phase intervals. Results figures below show the measured cumulative mean intensity values throughout all ETDRS areas of the macula. Each blue box within the dashed lines represents the range of intensity values for the healthy young control group. Horizontal lines in each box represent the mean intensity value. Outliers are represented by red plus signs. The cumulative mean intensity value for the VS participant is represented by the single horizontal red line in each ETDRS area.

In Figure 18A and 18B, we can see that throughout all the ETDRS areas of the macula, the cumulative mean intensity value is higher in the VS3 participant’s right eye (18A), and left eye (18B) compared to the PM cumulative mean intensity value of the healthy young control group. This was statistically significant in all ETDRS areas (* $p < 0.01$).

In Figure 19A and 19B, we can see that throughout all the ETDRS areas of the macula, the cumulative mean intensity value is higher in the VS4 participant’s right (19A), and left eye (19B) compared to the AM cumulative mean intensity value of the healthy young control group. This was statistically significant in all ETDRS areas (* $p < 0.01$).

In Figure 20A and 20B, we can see that throughout all the ETDRS areas of the macula, the cumulative mean intensity value is higher in the VS5 participant’s right (20A), and left eye (20B) compared to the PM cumulative mean intensity value of the healthy young control group. This was not statistically significant in the right eye but was statistically significant in all ETDRS areas in the left eye (* $p < 0.01$).

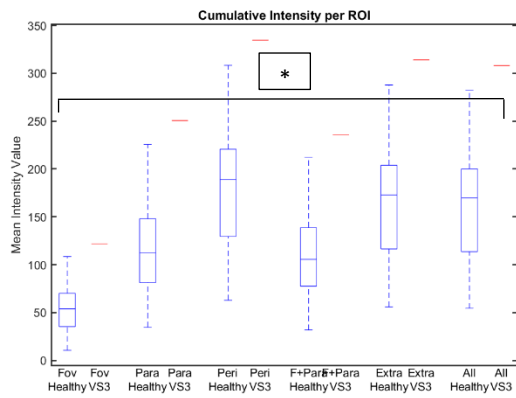
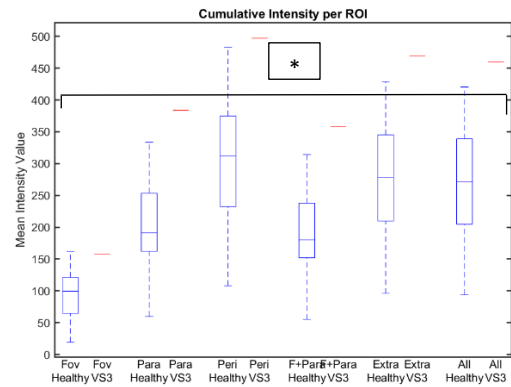
A**B**

Figure 18: The measured cumulative mean intensity values for the right (A) and left (B) eyes of VS3 (horizontal red lines) compared to PM mean intensity values of healthy young controls (horizontal line in blue boxes, n=31) throughout all ETDRS areas of the macula. The mean intensity levels are higher in VS3 in all areas of the macula (*p<0.01 in all ETDRS areas).

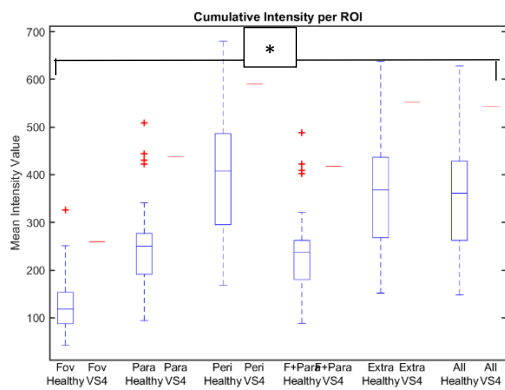
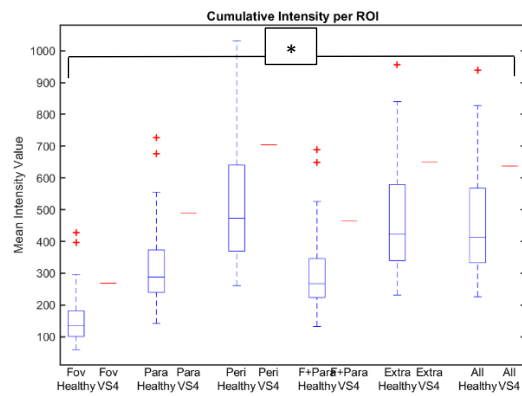
A**B**

Figure 19: The measured cumulative mean intensity values for the right (A) and left (B) eyes of VS4 compared to AM mean intensity values of healthy young controls (n=31) throughout all ETDRS areas of the macula. The mean intensity levels are higher in VS4 in all areas of the macula (*p<0.01 in all ETDRS areas).

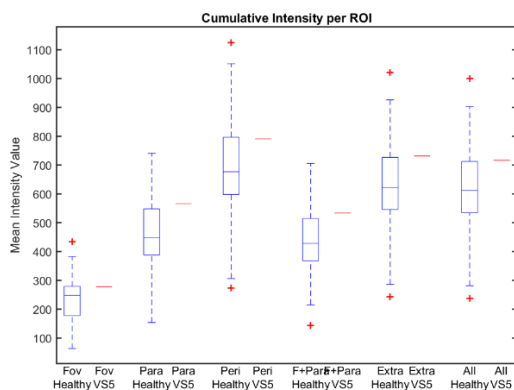
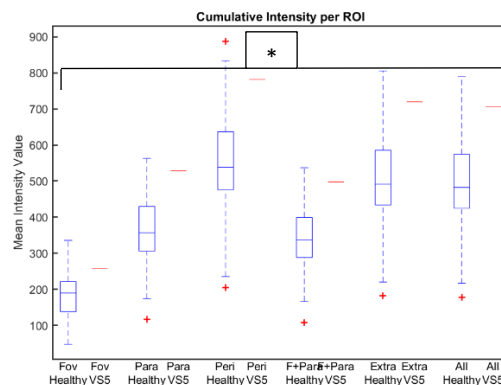
A**B**

Figure 20: The measured cumulative mean intensity values for the right (A) and left (B) eyes of VS5 compared to PM mean intensity values of healthy young controls (n=31) throughout all ETDRS areas of the macula. The mean intensity levels are higher in VS5 in all areas of the macula, NS for the right eye, statistically significant for the left eye (*p<0.01 in all ETDRS areas).

Due to relative rareness of this condition and the longitudinal nature of this study, two participants with VS symptoms recruited last year (VS1 and VS2) were also reanalysed using the new “features” based technique for FFA analysis using FOVAS and results compared to VS3,4 and 5. Similar data was obtained with the cumulative mean intensity values significantly higher in both eyes in both VS1 and VS2 (except for the perifovea in VS2 right eye) in all ETDRS areas (*p<0.01). Graphs not included.

With a sample size now of 5, grouped analysis, and not just individual analysis as above, of participants was now compared to the healthy young control group to assess the validity of increased fluorescein signal seen in individual results above. Due to the bilateral imaging technique in VS compared to the unilateral technique in the healthy young control group of the IRCP, cumulative analysis was not appropriate, but FFA phase analysis was compared between groups.

Figure 21 shows the grouped VS AM data (n=3) compared to the healthy young control data (n=31). This includes participants VS1, VS2 and VS4. The mean intensity values of VS and healthy young controls were compared at the early (0.5-2 mins), mid (2-6 mins) and late (6-10 mins) phases of FFA. All ETDRS regions of the macula demonstrate an increase in the mean fluorescein signal in the VS group compared to the healthy young controls. In the early phase no significant signal difference was seen. In the mid phase, a significantly increased fluorescein signal was seen in the fovea (*p<0.01) parafovea (*p<0.05), fovea+ parafovea regions when combined (*p<0.05), but NS overall and in other ETDRS areas. In the late phase, a significantly increased fluorescein signal was seen in the fovea (*p<0.01), parafovea (*p<0.05), fovea+parafovea (*p<0.05), and overall (*p<0.05). NS in other ETDRS areas.

Figure 22 shows the grouped VS PM data (n=2) compared to the healthy young control data (n=31). This includes participants VS3 and VS5. The mean intensity values between VS and

healthy young controls were compared at the early (0.5-2 mins), mid (2-6 mins) and late (6-10 mins) phases of FFA. All ETDRS regions of the macula demonstrate an increase in the mean fluorescein signal in the VS group compared to the healthy young controls. In the early phase, a significantly increased fluorescein signal was seen in all ETDRS areas (* $p < 0.05$). In the mid phase, no statistically increased fluorescein signal was seen in all ETDRS areas. In the late phase, a significantly increased fluorescein signal was seen in the parafovea (* $p < 0.05$), fovea+parafovea (* $p < 0.05$), and overall (* $p < 0.05$). NS in other ETDRS areas.

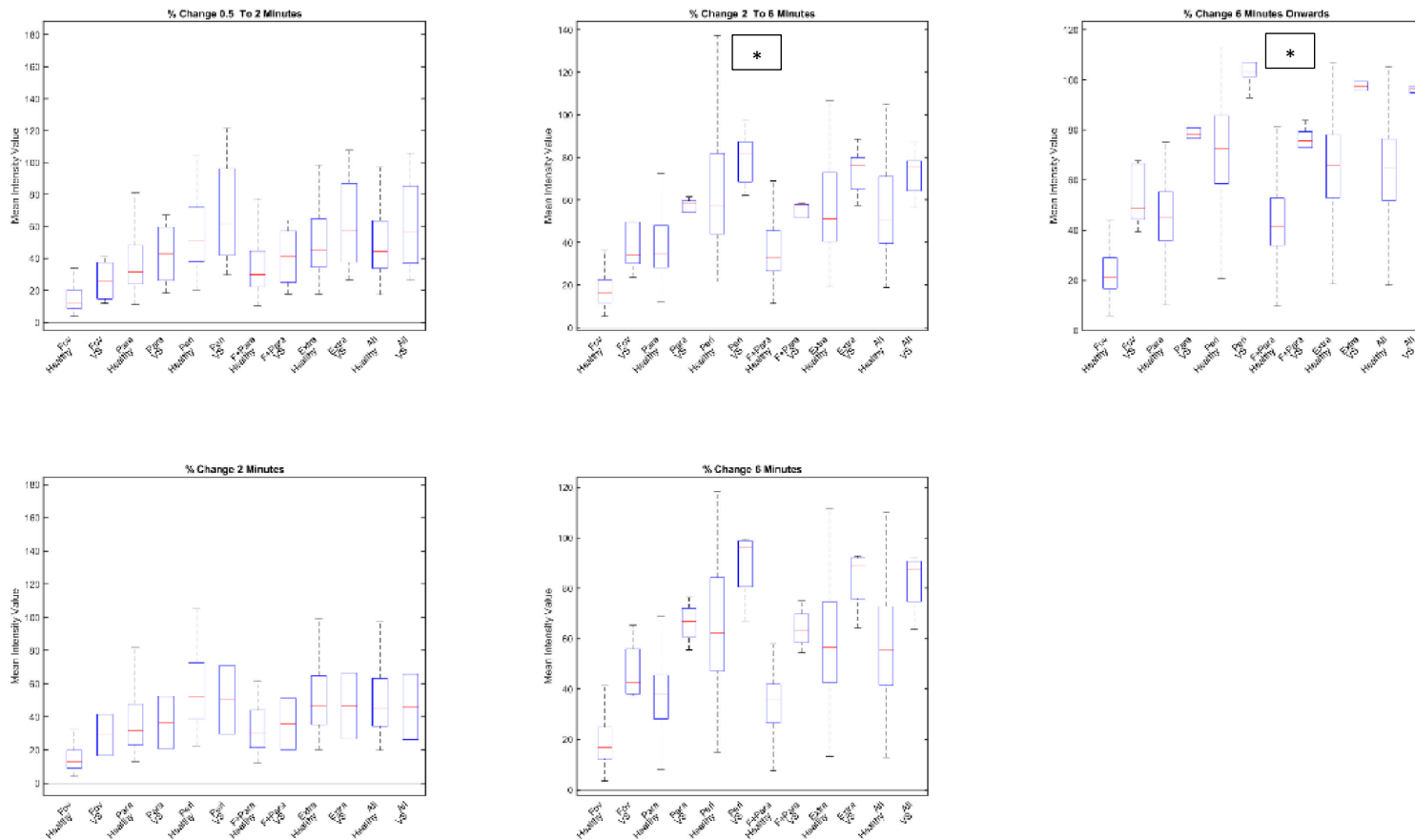


Figure 21: Grouped VS AM data (n=3) vs healthy young control data (n=31). The mean intensity values of VS and healthy young controls were compared at the early, mid, and late phases of FFA. All ETDRS regions of the macula demonstrate an increase in the mean fluorescein signal in the VS group compared to the healthy young controls. Early phase (NS), mid phase (significant in some regions, but not overall), late phase (significant overall).

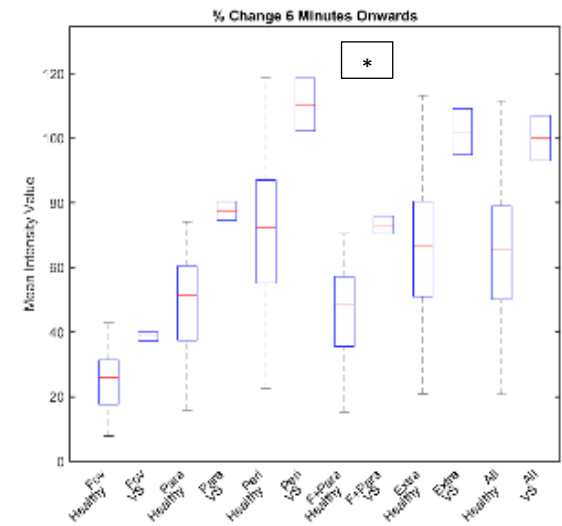
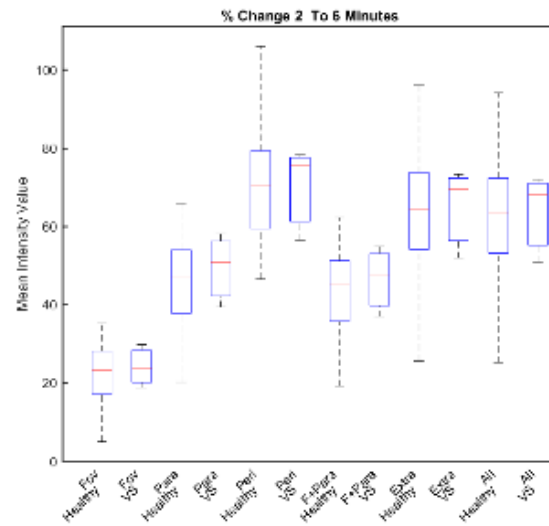
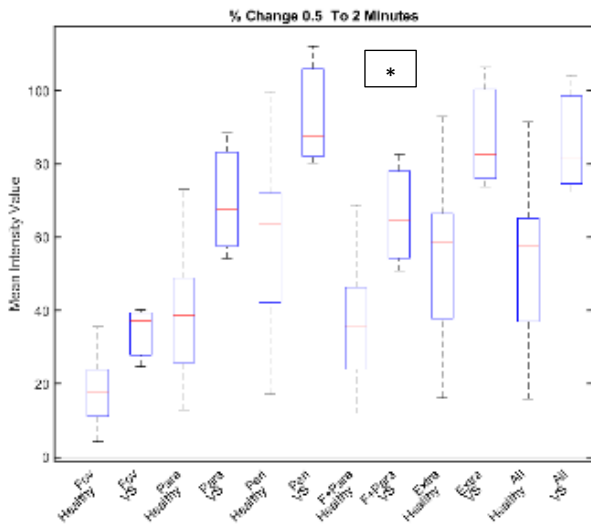


Figure 22: Grouped VS PM data (n=2) vs healthy young control data (n=31). The mean intensity values of VS and healthy young controls was compared at the early, mid, and late phases of FFA. All ETDRS regions of the macula demonstrate an increase in the mean fluorescein signal in the VS group compared to the healthy young controls. Early phase (all areas, significant), mid phase (NS), late phase (significant overall, and in some ETDRS areas).

DISCUSSION AND CONCLUSION

4.1 The AMD IRCP

AMD is the number one cause of central vision loss in those greater than 55 years, with a projected further increase in incidence over the coming decades due to an aging demographic worldwide [30]. Molecular mechanisms which influence progression from early (characterised by drusen deposits) to late-stage AMD remain unclear, and no effective treatment exists for GA.

The current thinking, holding widespread opinion, is that the initial dysfunction from normal homeostasis occurs in the oBRB and RPE leading to PR damage and finally geographic atrophy [36]. This research, in addition to previous studies within the Campbell lab, has demonstrated in both animal models and humans a role for iBRB dysfunction in AMD, with an attenuation or loss in circadian related cycling of inner retinal vasculature permeability [43]. We suggest that circadian regulated permeability of the iBRB is the main process which establishes the so called retinal interstitial kinesis or “current”, where TJs open just enough in the evening/overnight allowing diffusion of oxygen and nutrients to the PRs whilst simultaneously creating a diffusion current in the opposite direction back to the iBRB. This allows clearance of damaging metabolic products from the metabolically sensitive neural retina which diffuse back into the iBRB. These TJs then close again in the early/mid-morning preventing an overload of material to the retina, PRs and RPE. This cycle then repeats, thus facilitating a normal healthy circadian controlled retinal microenvironment.

We postulate that a chronic and size-selective disruption of the iBRB will lead to a downstream accumulation of metabolic debris and damaging species in the RPE over a prolonged period. Loss of TJ protein control, particularly claudin-5, could disrupt the normal retinal interstitial kinesis, resulting in the collection of damaging material in the retina, leading to RPE dysfunction, drusen formation and finally GA. Evidence for this has come from previous work where expression of the claudin-5 gene (*CLDN5*), controlled by the circadian clock and the transcription factor *BMAL1*, cycles in a circadian manner with lower expression levels in the evening versus the morning tissue samples [43]. Claudin-5 suppressed mice fed a fatty diet developed RPE dysfunction and atrophy [43]. In addition, other studies have demonstrated claudin-5 expression levels cycle in a circadian rhythm which are controlled by *BMAL1*, a component of the circadian clock [86,87]. The passive paracellular diffusion of material from the iBRB to the retinal tissue appears to be strongly controlled by Claudin-5 expression levels [86,87].

Similarly, increased permeability of the iBRB has been demonstrated in human and animal models of hypercholesterolemia and diabetes mellitus [88, 89]. These studies also demonstrated decreased levels of TJ protein expression, including claudin -5 and occludin [88-90]. Alterations of the retinal tissue consistent with clinical markers of these disease processes was also seen, including retinal layer thinning and the presence of plasma proteins in the retinal parenchyma [88-90]. In addition, similar findings were seen in in the BBB and cerebral cortex

in a porcine model [88]. It is tempting to postulate similar disease processes are taking place in both the iBRB and BBB due to their structural and functional similarities as outlined in the introduction section.

Other TJ proteins are also under the influence of the circadian clock and may also play a role in blood tissue barrier integrity. The MARVEL proteins (occludin, tricellulin and marvelD3), the transmembrane Junctional Adhesion Molecules (JAMs), and the cytoplasmic scaffolding proteins Zonula Occludens (ZO's) are all important TJ proteins [75]. However, contrasting evidence has been seen with Occludin where Occludin deficient mice still formed viable blood tissue barriers in one study [76], whereas in another study involving the BBB of wild type mice, Occludin mRNA levels were shown to oscillate in a 24-hour manner [77]. This expression pattern was lost in mice who had circadian clock gene disruption and a subsequent breakdown in BBB integrity was demonstrated [77].

In addition, the other TJ proteins described may be more important in maintaining other tissue barriers outside of the BBB and BRB. For example, the circadian regulation of Occludin and Claudin-1 expression in the colon epithelium was demonstrated to play a vital role in colon permeability, integrity, and colitis when expression level of these proteins was low [78]. There is currently a paucity of evidence examining the role of circadian regulation of other TJ proteins in the BRB.

Analysis of FFA images from the young healthy control group has revealed a dynamic iBRB with prolonged fluorescein signal in the macular retinal parenchyma in the evening compared to the morning. These results along with findings from AMD and age matched control participants provide strong evidence that disruption of the circadian derived iBRB interstitial kinesis may contribute to the initial AMD disease process.

We have established that there is an increased mean intensity fluorescein signal in the PM compared to the AM in all ETDRS areas of the macula in the healthy young control group (Figures 6 and 7). This higher PM mean intensity fluorescein signal is strongest at the mid phase (2-6mins) in all ETDRS areas of the macula and the late phase (6-10 mins) at the fovea in healthy young controls (Figure 8). There is an increased mean intensity PM vs AM signal during the early phase (0.5-2 mins), however this was not statistically significant. These findings again suggest that there is a more "intact" iBRB in the morning compared to the evening. The higher PM signal seen in the mid phase and late phase (as opposed to the early phases) may be due to fluorescein dynamics and a more permeable iBRB in the evening, which we believe is a normal phenomenon. It takes time for sodium fluorescein to leave the inner retinal blood vessels and deposit in the retinal parenchyma, therefore, during the early phase of FFA, no significant difference in mean intensity values was seen between the AM and PM. As the FFA moves to the later phases, increased levels of sodium fluorescein then can leave the more permeable iBRB in the PM relative to the AM, illustrated by the increased percentage difference of mean intensity values observed during the mid-phase and late phase of the FFA.

We can see that in the age matched control cohort there was an increased mean cumulative intensity value in the PM vs AM in certain ETDRS areas of the macula (parafovea, perifovea, fovea and parafovea), however this was not significant and other areas (fovea and extrafovea) showed no increase in cumulative mean intensity in PM vs AM (Figure 9). In addition, there

was an increased mean signal intensity percentage difference in the PM compared to the AM at all ETDRS areas of the macula (except for the fovea) (Figure 10). However, this increase was not statistically significant. This contrasts with the increased mean cumulative intensity values and increased percentage differences in the PM vs AM seen in the healthy young control group. It is likely that the circadian regulation of iBRB permeability is present in age matched controls (aged >65 years) but is reduced in comparison to younger people. One theory to explain this, is that changes in circadian rhythm occur as we age, in addition to poorer sleep duration and quality, which may account for the reduced PM vs AM signal differential, but not the complete disappearance of it as we saw in the AMD group.

Another factor to consider for this statistical outcome is the smaller participant number (n=13) compared to the AMD and healthy young control groups. The power calculations for this study expect an n number of at least twenty to compare accurately with the other two study groups, which will increase in future years.

In the AMD group, quantification of the fluorescein signal differential within different ETDRS zones of the macula demonstrated no increased fluorescein signal in the PM compared to the AM (Figures 11 and 12). This again contrasts with the healthy young control group where the mean intensity signal was significantly increased at the fovea, parafovea, and fovea+parafovea in the PM compared to the AM. This also contrasts to the age matched control group where the mean signal intensity percentage difference was visibly higher in the PM compared to the AM, but not as a large a difference compared to the healthy young controls, as evidenced by the “not significant” statistical result. Taken together, this suggests that the circadian regulation of iBRB permeability is lost in early-stage AMD participants and that the barrier does not close in the morning like in healthy young controls (who have a lower fluorescein signal in AM) but remains open in both the PM and AM allowing the same level of fluorescein to diffuse out of the vasculature at both timepoints and likely throughout a 24-hour period. It appears that older persons greater than 65 years without clinical signs of AMD also have some dysregulation of their circadian controlled iBRB barrier function as previously discussed. However, a higher “n” number in the age matched control group is needed to fully justify this claim.

Further evidence of this barrier dysfunction in AMD participants comes from the FFA phase analysis results (Figure 13). We have seen in the healthy young control group a significantly higher mean intensity signal in the PM compared to the AM during the mid-phase and late phase at the fovea with no significant differences seen during the other phases during FFA (Figure 8). In contrast, a reversal is seen during the mid-phase in the AMD group, where a higher mean intensity fluorescein signal is seen in the AM compared to the PM. Taken together, this illustrates the lack of iBRB function in AMD during the mid-phase of FFA where fluorescein is abnormally leaking out at both AM and PM and may be extravasating more during the morning time. In addition, the higher PM vs AM signal seen at 6 minutes in AMD group may be explained by prolonged fluorescein signal at the macula in the PM. This may reflect a difficulty in fluorescein molecules diffusing back into the iBRB from the inner retinal layers as they are “fighting” to try and overcome the concentration gradient of the chronically open iBRB throughout the day and evening. In healthy young controls during the late phase no signal differential was seen, thereby suggesting that fluorescein can diffuse out but can then

diffuse back into the iBRB and be removed from the macula due to the functioning interstitial retinal kinesis.

Finally, when mean cumulative fluorescein signal intensity was compared between healthy young controls and AMD participants clear differences were seen (Figure 14). In the morning, increased mean intensity was seen in the AMD group compared to the young control group. This contrasts with evening findings, where increased fluorescein signal intensity was seen in the healthy young control group compared to the AMD group. Taken together, this further illustrates the loss of circadian cycling and retinal interstitial kinesis in the AMD group. In young controls the circadian mediated effect of higher fluorescein signal in the evening compared to the morning is evident thus suggesting the natural kinesis is present in this group. This is completely reversed in the AMD group, where a higher mean intensity signal is seen in the morning when compared to healthy young controls. Even though the “mean intensity value” on the y axis may be difficult to compare between the morning and evening graphs, the mean intensity level in each ETDRS area in the AMD group appears similar in value across both the AM and PM graphs (Figure 14, compare AMD AM and PM values).

This indicates that a constant level of fluorescein is measured at the macula in both the morning and evening, therefore suggesting that a constant “leaky” iBRB is present allowing a constant influx of material to the inner retina. This also may explain the increased fluorescein signal in the PM seen at 6 minutes during phase analysis in the AMD group (Figure 13). The constant extravasation of fluorescein throughout the day may make clearance more difficult and hence a higher mean intensity value is seen at the late phase PM values in the AMD group. We think that this also occurs with other molecules/material that are moving out of the iBRB and “sitting” in the inner retinal layers and are slow or cannot diffuse back into the inner retinal blood vessels, hence causing continuous low-level damage to the PR’s and then secondary RPE dysfunction.

Future directions:

We have now defined a “normal distribution” of fluorescein signal in a healthy young control group with a natural increased signal in all ETDRS areas of the macula in the evening compared to the morning. The use of FOVAS as a screening tool in other at-risk cohorts (not just early-stage AMD) to assess circadian rhythm dysfunction is now a real possibility. For example, the screening of patients with diseases known to have an element of iBRB dysfunction (eg. diabetic retinopathy) for circadian rhythm changes may provide insight into whether a circadian mediated dysfunction in the iBRB is present in these diseases. In addition, by expanding the age matched control cohort, elderly patients could be screened for circadian rhythm dysfunction before clinical signs of AMD develop and thus take steps to restore the body’s natural circadian rhythm and prevent disease onset. Increased sleep, reduced blue light exposure before sleep, daily exercise, and exposure to daylight have all been proven to aid natural circadian cycles [64, 65].

It is tempting to contemplate on future therapeutic targets and the role FOVAS may play in measuring outcome. For example, could an AMD participant with a disrupted circadian

fluorescein signal be given a therapeutic agent restoring the TJs of endothelial cells to a cyclical manner thus restoring the circadian mediated fluorescein signal to that of a healthy young control participant proving treatment response and a risk reduction or even reversal of AMD progression?

As the sample size increases, further work should examine FOVAS results by AMD subgroup (i.e., Grade 2,3 and 4) and expand to include all grades of AMD including GA and neovascular AMD. This would be interesting to see, as iBRB cycling may be better preserved in those with an earlier stage of the disease, and may be further disrupted in those with wet AMD and GA.

Future studies within the Campbell lab aim to analyse DNA, RNA and serum collected from participants and correlate these findings with imaging results. RNA levels of BMAL-1, Per2 and Rev-alpha will be analysed for each participant. These are key circadian rhythm associated proteins which act through a negative feedback system to control circadian associated gene expression [71]. Genetic susceptibility also has a central role in the development and progression of AMD in an individual. Several gene variants are known to increase susceptibility to AMD [72]. The most important ones identified to date include the complement system (CFH, CFB, C3 and CFI) involved during the inflammatory cycle in AMD, lipid metabolism (APOE), and cell survival pathways including stress response and apoptosis (ARMS2) [72,73]. Melatonin and cortisol levels, which are also influenced by the circadian clock will be analysed. There is some evidence that changes in timing and concentration of these hormones can lead to impaired phagocytosis and clearance of damaged PRs, accumulation of harmful metabolites including lipofuscin in the RPE, and thus AMD pathogenesis [74].

The findings from these samples will then be correlated with FOVAS fluorescein signal values from the same participant and compared between the healthy young control, age matched control and AMD groups for any correlation in findings. In addition, as the sample size increases, subgroup analysis involving the different grades of AMD could be statistically performed. Could it be possible that fluorescein signal intensity is linked to AMD genetic risk variants, circadian clock transcript expression or serum cortisol/melatonin levels?

Conclusion

In conclusion, these findings suggest that the iBRB is highly dynamic, with increased fluorescein permeability in the evening compared to the morning in young healthy controls. The circadian associated fluorescein signal differential present in young healthy controls appears attenuated in age matched controls, with no significant difference present in AMD subjects. This suggests that the circadian dependant regulation of iBRB kinesis decreases with ageing and is arrested in AMD. We suggest that this disruption may be due to decreased expression or dysfunction of the TJ protein claudin-5 resulting in a more open, "leakier" iBRB, which may be one of the early initiating factors in AMD pathogenesis.

4.2 VS

Visual snow is a novel neurological condition defined by the subjective description of constant positive visual phenomenon in both eyes [53]. Typically described as a “static background” in addition to other visual symptoms such as “floaters” and flashing light phenomenon [53, 54]. Intraocular pathology is not present, and some studies have suggested aberrant processing in the visual cortex and associated cortical structures as an explanation [55,56,58].

Given the similarities between the BBB and iBRB as previously discussed, and the evolving evidence that neurological conditions involving dysfunction of the BBB may also involve dysfunction and loss of integrity of the iBRB, several participants with subjective visual snow symptoms were recruited and the iBRB integrity analysed and compared to the healthy young control group from the IRCP using FFA and FOVAS.

Using FOVAS, we have demonstrated an increased fluorescein signal at the macula in all VS participants analysed, indicating a more permeable iBRB may be present in this condition. However, as the cumulative mean intensity value from each individual VS participant was compared to the cumulative mean intensity value from the healthy young control group of 31 participants, statistical significance may be less likely. For example, each VS participant may be an outlier, and this increased fluorescein intensity signal in each VS participant may be at the upper scale of normal of the healthy young control group.

However, as each VS participant was under 35 years old, it is more likely the hyperfluorescence seen is a significant finding, as an increased cumulative mean intensity value vs the healthy young control group was evident in all ETDRS areas, in both left and right eyes, and in each participant. As a result, it appears unlikely that these findings are not statistically significant, and it will be interesting to see if the results remain similar as the total number of visual snow participants increases. Future effort should aim to increase participant numbers, as stronger grouped analysis could then be performed and compared to the healthy young control AM and PM mean intensity values for statistical significance.

In addition, when reviewing mean intensity values during different phases of the FFA (early, mid, and late phase, not reported), increased mean intensity values were observed in each VS participant compared to healthy young controls. This varied however between individuals both at different phases of the FFA and in ETDRS area. Nonetheless, these findings point to some merit in expanding the VS participant number and examining percentage changes in the mean intensity values compared to the healthy young control group during phase analysis.

No grossly abnormal ocular findings were seen in any VS participants that may have been responsible for their visual phenomena. Bilateral lattice degeneration in the retinal was seen on fundus examination in VS3, but the patient reported high myopia, a common finding in this cohort. Bilateral silver wiring of the retinal arterioles was seen in VS5, indicative of vessel wall thickening from chronic hypertension. Normal ocular findings have been reported in a VS cohort and other case studies following ocular assessment and examination, making it unlikely that the clinically detectable pathology is the primary cause of VS [71].

Cortical spreading depression (CSD) is characterised by a wave of neuron and glial cell depolarisation within the cortex and other anatomical brain locations [66]. It is one of the main theories behind migraine pathophysiology and correlates with the onset of migraine aura (positive visual or auditory phenomenon experienced by many before the onset of

headache)[79]. This wave of depolarisation is associated with blood flow changes in the cortex and opening of the BBB transiently, thought to lead to vasoactive peptide release, activation of nociceptors and the onset of clinical signs of pain, i.e., migraine headache [67].

CSD has also been implicated in VS pathology with some distinct but probably similar neural pathways as in migraine [68]. An association with migraine was also present in the current study, as despite the small sample size, two participants reported suffering from migraine. In another study increased fluorodeoxyglucose (FDG)-positron emission tomography (PET) metabolism was noted in VS patients compared to controls in certain brain areas [69] and a more generalised increased cerebral blood flow when compared to controls [70]. This again highlights the BBB changes and neuronal transmission changes taking place during VS.

Therefore, due to the likely more permeable BBB in VS and the similarities between the BBB and iBRB, it is feasible that a more permeable iBRB is present in VS as evidenced from the FOVAS results. Whether this contributes to VS symptoms or is an incidental finding due to the molecular similarities between the two barrier systems remains to be determined.

However, it is interesting to speculate that increased/abnormal neuronal cell excitability in the retina, like in visual cortex and other anatomical areas in the brain during VS and migraine, may also lead to chronic changes in iBRB blood vessel integrity, resulting in a more permeable iBRB. This may explain the increased fluorescein signal seen at the macula in VS and perhaps lead some way to explain the presence of the unique visual phenomenon seen in VS.

In VS5, the discrepancy between statistically significant increased mean intensity fluorescein signal in the left eye and increased, but not significant in the right eye when compared to healthy young controls is difficult to explain. Out of focus images cause the surrounding pixels of a bright object to appear brighter than they truly are, hence, the average signal for an image would be higher than it should be. However, for VS5, FFA image quality was good in both eyes. Again, a larger sample size can help validate any individual findings. Unfortunately, FFA images were out of focus in both right and left eyes in VS3, perhaps discounting the statistically increased fluorescein signal recorded for VS3 individual analysis and falsely elevating the increased mean intensity signal seen in grouped PM analysis (as VS3 was part of the PM group). However, the strong statistical findings of increased fluorescein signal of the four other VS participants during individual analysis makes it unlikely that VS3 was the only outlier.

Interesting findings are seen in FFA phase analysis results where grouped VS AM and grouped VS PM data were compared to the IRCP healthy young control AM and PM data, respectively. In the AM analysis, intensity signals of fluorescein are similar in early phase, some increased signal seen in the fovea and parafovea but not overall in the mid phase, and a clear increase in signal is seen overall and in most ETDRS regions in the late phase (Figure 21). These findings are in line with what we would expect if increased iBRB permeability was present. As the time passes during FFA to 6 minutes onwards, more and more fluorescein has the time and opportunity to leave the “leaky” inner retinal blood vessels compared to earlier phases and accumulate in the retinal parenchyma (like findings seen in FOVAS analysis of the late phases of the healthy young control group). There is now a statistically significant increased concentration of fluorescein in the retinal parenchyma of the macula that is measurably different to healthy young controls.

Despite the small sample size (n=3), this correlates well with the hypothesis that the iBRB vessels may be more permeable in VS and provides an additional theory for the cause of VS, in addition to the cerebral vasculature and aberrant neuronal firing pathway theories as outlined above.

In the PM analysis, intensity signals of fluorescein are statistically increased in the early phase of the VS group compared to the healthy young control group. No significant difference is seen in the mid phase, and a clear increase in signal is seen overall and in some ETDRS regions in the late phase (Figure22). These findings are more difficult to interpret than AM grouped analysis for two reasons. Firstly, the small n number of two makes it more likely that an outlier in a small group can skew the overall trend in that group, and secondly, when actual individual FFA images were reviewed, the VS3 participant had out of focus images for most timepoints, thereby perhaps skewing the statistical analysis as this participant made up 50% of the group.

Conclusion

Overall, these findings demonstrate that the iBRB may be more permeable in people reporting visual snow symptoms. Future studies should increase the numbers for both AM and PM grouped analysis to validate these findings. More consideration may need to be given for the role the retina may play in VS pathogenesis. Electrophysiology studies of the retina may need to be performed.

References

1. Country, M. W. (2017) Retinal metabolism: A comparative look at energetics in the retina, *Brain Res.* 1672, 50-57.
2. Guymer, R. H., Bird, A. C. & Hageman, G. S. (2004) Cytoarchitecture of choroidal capillary endothelial cells, *Invest Ophthalmol Vis Sci.* 45, 1660-6.
3. Sun, Y. & Smith, L. E. H. (2018) Retinal Vasculature in Development and Diseases, *Annu Rev Vis Sci.* 4, 101-122.
4. Cunha-Vaz, J., Bernardes, R. & Lobo, C. (2011) Blood-retinal barrier, *Eur J Ophthalmol.* 21 Suppl 6, S3-9.
5. Booi, J. C., Baas, D. C., Beisekeeva, J., Gorgels, T. G. & Bergen, A. A. (2010) The dynamic nature of Bruch's membrane, *Prog Retin Eye Res.* 29, 1-18.
6. Hussain, A. A., Starita, C., Hodgetts, A. & Marshall, J. (2010) Macromolecular diffusion characteristics of ageing human Bruch's membrane: implications for age-related macular degeneration (AMD), *Exp Eye Res.* 90, 703-10.
7. Tisi, A., Feligioni, M., Passacantando, M., Ciancaglini, M. & Maccarone, R. (2021) The Impact of Oxidative Stress on Blood-Retinal Barrier Physiology in Age-Related Macular Degeneration, *Cells.* 10.
8. Strauss, O. (2005) The retinal pigment epithelium in visual function, *Physiol Rev.* 85, 845-81.
9. Sparrow, J. R., Hicks, D. & Hamel, C. P. (2010) The retinal pigment epithelium in health and disease, *Curr Mol Med.* 10, 802-23.
10. Marneros, A. G., Fan, J., Yokoyama, Y., Gerber, H. P., Ferrara, N., Crouch, R. K. & Olsen, B. R. (2005) Vascular endothelial growth factor expression in the retinal pigment epithelium is essential for choriocapillaris development and visual function, *Am J Pathol.* 167, 1451-9.
11. Simo, R., Villarreal, M., Corraliza, L., Hernandez, C. & Garcia-Ramirez, M. (2010) The retinal pigment epithelium: something more than a constituent of the blood-retinal barrier--implications for the pathogenesis of diabetic retinopathy, *J Biomed Biotechnol.* 2010, 190724.
12. Hormel, T. T., Jia, Y., Jian, Y., Hwang, T. S., Bailey, S. T., Pennesi, M. E., Wilson, D. J., Morrison, J. C. & Huang, D. (2021) Plexus-specific retinal vascular anatomy and pathologies as seen by projection-resolved optical coherence tomographic angiography, *Prog Retin Eye Res.* 80, 100878.
13. Nian, S., Lo, A. C. Y., Mi, Y., Ren, K. & Yang, D. (2021) Neurovascular unit in diabetic retinopathy: pathophysiological roles and potential therapeutical targets, *Eye Vis (Lond).* 8, 15.
14. Gardner, T. W. & Davila, J. R. (2017) The neurovascular unit and the pathophysiological basis of diabetic retinopathy, *Graefes Arch Clin Exp Ophthalmol.* 255, 1-6.
15. Frank, R. N., Turczyn, T. J. & Das, A. (1990) Pericyte coverage of retinal and cerebral capillaries, *Invest Ophthalmol Vis Sci.* 31, 999-1007.
16. Trost, A., Lange, S., Schroedl, F., Bruckner, D., Motloch, K. A., Bogner, B., Kaser-Eichberger, A., Strohmaier, C., Runge, C., Aigner, L., Rivera, F. J. & Reitsamer, H. A. (2016) Brain and Retinal Pericytes: Origin, Function and Role, *Front Cell Neurosci.* 10, 20.
17. Newman, E. A. (2015) Glial cell regulation of neuronal activity and blood flow in the retina by release of gliotransmitters, *Philos Trans R Soc Lond B Biol Sci.* 370.
18. Abbott, N. J., Ronnback, L. & Hansson, E. (2006) Astrocyte-endothelial interactions at the blood-brain barrier, *Nat Rev Neurosci.* 7, 41-53.

19. Fresta, C. G., Fidilio, A., Caruso, G., Caraci, F., Giblin, F. J., Leggio, G. M., Salomone, S., Drago, F. & Bucolo, C. (2020) A New Human Blood-Retinal Barrier Model Based on Endothelial Cells, Pericytes, and Astrocytes, *Int J Mol Sci.* 21.
20. Vecino, E., Rodriguez, F. D., Ruzafa, N., Pereiro, X. & Sharma, S. C. (2016) Glia-neuron interactions in the mammalian retina, *Prog Retin Eye Res.* 51, 1-40.
21. Shin, K., Fogg, V. C. & Margolis, B. (2006) Tight junctions and cell polarity, *Annu Rev Cell Dev Biol.* 22, 207-35.
22. Klaassen, I., Van Noorden, C. J. & Schlingemann, R. O. (2013) Molecular basis of the inner blood-retinal barrier and its breakdown in diabetic macular edema and other pathological conditions, *Prog Retin Eye Res.* 34, 19-48.
23. Dejana, E. (2004) Endothelial cell-cell junctions: happy together, *Nat Rev Mol Cell Biol.* 5, 261-70.
24. Rizzolo, L. J., Peng, S., Luo, Y. & Xiao, W. (2011) Integration of tight junctions and claudins with the barrier functions of the retinal pigment epithelium, *Prog Retin Eye Res.* 30, 296-323.
25. Colegio, O. R., Van Itallie, C. M., McCrea, H. J., Rahner, C. & Anderson, J. M. (2002) Claudins create charge-selective channels in the paracellular pathway between epithelial cells, *Am J Physiol Cell Physiol.* 283, C142-7.
26. Nitta, T., Hata, M., Gotoh, S., Seo, Y., Sasaki, H., Hashimoto, N., Furuse, M. & Tsukita, S. (2003) Size-selective loosening of the blood-brain barrier in claudin-5-deficient mice, *J Cell Biol.* 161, 653-60.
27. Greene, C., Hanley, N. & Campbell, M. (2019) Claudin-5: gatekeeper of neurological function, *Fluids Barriers CNS.* 16, 3.
28. Argaw, A. T., Gurfein, B. T., Zhang, Y., Zameer, A. & John, G. R. (2009) VEGF-mediated disruption of endothelial CLN-5 promotes blood-brain barrier breakdown, *Proc Natl Acad Sci U S A.* 106, 1977-82.
29. Muthusamy, A., Lin, C. M., Shanmugam, S., Lindner, H. M., Abcouwer, S. F. & Antonetti, D. A. (2014) Ischemia-reperfusion injury induces occludin phosphorylation/ubiquitination and retinal vascular permeability in a VEGFR-2-dependent manner, *J Cereb Blood Flow Metab.* 34, 522-31.
30. Wong, W. L., Su, X., Li, X., Cheung, C. M., Klein, R., Cheng, C. Y. & Wong, T. Y. (2014) Global prevalence of age-related macular degeneration and disease burden projection for 2020 and 2040: a systematic review and meta-analysis, *Lancet Glob Health.* 2, e106-16.
31. Mitchell, P., Liew, G., Gopinath, B. & Wong, T. Y. (2018) Age-related macular degeneration, *Lancet.* 392, 1147-1159.
32. Lambert, N. G., ElShelmani, H., Singh, M. K., Mansergh, F. C., Wride, M. A., Padilla, M., Keegan, D., Hogg, R. E. & Ambati, B. K. (2016) Risk factors and biomarkers of age-related macular degeneration, *Prog Retin Eye Res.* 54, 64-102.
33. Fleckenstein, M., Keenan, T. D. L., Guymer, R. H., Chakravarthy, U., Schmitz-Valckenberg, S., Klaver, C. C., Wong, W. T. & Chew, E. Y. (2021) Age-related macular degeneration, *Nat Rev Dis Primers.* 7, 31.
34. Hernandez-Zimbron, L. F., Zamora-Alvarado, R., Ochoa-De la Paz, L., Velez-Montoya, R., Zenteno, E., Gullias-Canizo, R., Quiroz-Mercado, H. & Gonzalez-Salinas, R. (2018) Age-Related Macular Degeneration: New Paradigms for Treatment and Management of AMD, *Oxid Med Cell Longev.* 2018, 8374647.
35. Age-Related Eye Disease Study Research, G. (2001) A randomized, placebo-controlled, clinical trial of high-dose supplementation with vitamins C and E, beta carotene, and zinc for age-related macular degeneration and vision loss: AREDS report no. 8, *Arch Ophthalmol.* 119, 1417-36.

36. Sparrow, J. R. & Duncker, T. (2014) Fundus Autofluorescence and RPE Lipofuscin in Age-Related Macular Degeneration, *J Clin Med.* 3, 1302-21.
37. Shu, D. Y., Butcher, E. & Saint-Geniez, M. (2020) EMT and EndMT: Emerging Roles in Age-Related Macular Degeneration, *Int J Mol Sci.* 21.
38. Murali, A., Krishnakumar, S., Subramanian, A. & Parameswaran, S. (2020) Bruch's membrane pathology: A mechanistic perspective, *Eur J Ophthalmol.* 30, 1195-1206.
39. Adhi, M., Lau, M., Liang, M. C., Waheed, N. K. & Duker, J. S. (2014) Analysis of the thickness and vascular layers of the choroid in eyes with geographic atrophy using spectral-domain optical coherence tomography, *Retina.* 34, 306-12.
40. Wakatsuki, Y., Shinojima, A., Kawamura, A. & Yuzawa, M. (2015) Correlation of Aging and Segmental Choroidal Thickness Measurement using Swept Source Optical Coherence Tomography in Healthy Eyes, *PLoS One.* 10, e0144156.
41. Schultz, H., Song, Y., Baumann, B. H., Kapphahn, R. J., Montezuma, S. R., Ferrington, D. A. & Dunaief, J. L. (2019) Increased serum proteins in non-exudative AMD retinas, *Exp Eye Res.* 186, 107686.
42. Buschini, E., Piras, A., Nuzzi, R. & Vercelli, A. (2011) Age related macular degeneration and drusen: neuroinflammation in the retina, *Prog Neurobiol.* 95, 14-25.
43. Hudson, N., Celkova, L., Hopkins, A., Greene, C., Storti, F., Ozaki, E., Fahey, E., Theodoropoulou, S., Kenna, P. F., Humphries, M. M., Curtis, A. M., Demmons, E., Browne, A., Liddie, S., Lawrence, M. S., Grimm, C., Cahill, M. T., Humphries, P., Doyle, S. L. & Campbell, M. (2019) Dysregulated claudin-5 cycling in the inner retina causes retinal pigment epithelial cell atrophy, *JCI Insight.* 4.
44. Cahill, M. T., Mruthyunjaya, P., Bowes Rickman, C. & Toth, C. A. (2005) Recurrence of retinal pigment epithelial changes after macular translocation with 360 degrees peripheral retinectomy for geographic atrophy, *Arch Ophthalmol.* 123, 935-8.
45. Dierickx, P., Van Laake, L. W. & Geijsen, N. (2018) Circadian clocks: from stem cells to tissue homeostasis and regeneration, *EMBO Rep.* 19, 18-28.
46. Kofuji, P., Mure, L. S., Massman, L. J., Purrier, N., Panda, S. & Engeland, W. C. (2016) Intrinsically Photosensitive Retinal Ganglion Cells (ipRGCs) Are Necessary for Light Entrainment of Peripheral Clocks, *PLoS One.* 11, e0168651.
47. He, J., Hsuchou, H., He, Y., Kastin, A. J., Wang, Y. & Pan, W. (2014) Sleep restriction impairs blood-brain barrier function, *J Neurosci.* 34, 14697-706.
48. Kugler, E. C., Greenwood, J. & MacDonald, R. B. (2021) The "Neuro-Glial-Vascular" Unit: The Role of Glia in Neurovascular Unit Formation and Dysfunction, *Front Cell Dev Biol.* 9, 732820.
49. London, A., Benhar, I. & Schwartz, M. (2013) The retina as a window to the brain-from eye research to CNS disorders, *Nat Rev Neurol.* 9, 44-53.
50. Subirada, P. V., Paz, M. C., Ridano, M. E., Lorenc, V. E., Vaglienti, M. V., Barcelona, P. F., Luna, J. D. & Sanchez, M. C. (2018) A journey into the retina: Muller glia commanding survival and death, *Eur J Neurosci.* 47, 1429-1443.
51. Moss, H. E. (2015) Retinal Vascular Changes are a Marker for Cerebral Vascular Diseases, *Curr Neurol Neurosci Rep.* 15, 40.
52. Lasta, M., Pemp, B., Schmidl, D., Boltz, A., Kaya, S., Palkovits, S., Werkmeister, R., Howorka, K., Popa-Cherecheanu, A., Garhofer, G. & Schmetterer, L. (2013) Neurovascular dysfunction precedes neural dysfunction in the retina of patients with type 1 diabetes, *Invest Ophthalmol Vis Sci.* 54, 842-7.
53. Puledda, F., Schankin, C. & Goadsby, P. J. (2020) Visual snow syndrome: A clinical and phenotypical description of 1,100 cases, *Neurology.* 94, e564-e574.
54. Schankin, C. J., Maniyar, F. H., Digre, K. B. & Goadsby, P. J. (2014) 'Visual snow' - a disorder distinct from persistent migraine aura, *Brain.* 137, 1419-28.

55. Eren, O., Rauschel, V., Ruscheweyh, R., Straube, A. & Schankin, C. J. (2018) Evidence of dysfunction in the visual association cortex in visual snow syndrome, *Ann Neurol.* 84, 946-949.
56. Denuelle, M., Bouulloche, N., Payoux, P., Fabre, N., Trotter, Y. & Geraud, G. (2011) A PET study of photophobia during spontaneous migraine attacks, *Neurology.* 76, 213-8.
57. Schankin, C. J., Maniyar, F. H., Sprenger, T., Chou, D. E., Eller, M. & Goadsby, P. J. (2014) The relation between migraine, typical migraine aura and "visual snow", *Headache.* 54, 957-66.
58. Yoo, Y. J., Yang, H. K., Choi, J. Y., Kim, J. S. & Hwang, J. M. (2020) Neuro-ophthalmologic Findings in Visual Snow Syndrome, *J Clin Neurol.* 16, 646-652.
59. Bird, A. C., Bressler, N. M., Bressler, S. B., Chisholm, I. H., Coscas, G., Davis, M. D., de Jong, P. T., Klaver, C. C., Klein, B. E., Klein, R. & et al. (1995) An international classification and grading system for age-related maculopathy and age-related macular degeneration. The International ARM Epidemiological Study Group, *Surv Ophthalmol.* 39, 367-74.
60. Connolly, E., Rhatigan, M., O'Halloran, A. M., Muldrew, K. A., Chakravarthy, U., Cahill, M., Kenny, R. A. & Doyle, S. L. (2018) Prevalence of age-related macular degeneration associated genetic risk factors and 4-year progression data in the Irish population, *Br J Ophthalmol.* 102, 1691-1695.
61. Ryu, H., Joo, E. Y., Choi, S. J. & Suh, S. (2018) Validation of the Munich ChronoType Questionnaire in Korean Older Adults, *Psychiatry Investig.* 15, 775-782.
62. Roenneberg, T., Kuehnle, T., Juda, M., Kantermann, T., Allebrandt, K., Gordijn, M. & Merrow, M. (2007) Epidemiology of the human circadian clock, *Sleep Med Rev.* 11, 429-38.
63. Arora, R., Bellamy, H. & Austin, M. (2014) Applanation tonometry: a comparison of the Perkins handheld and Goldmann slit lamp-mounted methods, *Clin Ophthalmol.* 8, 605-10.
64. Tosini, G., Ferguson, I. & Tsubota, K. (2016) Effects of blue light on the circadian system and eye physiology, *Mol Vis.* 22, 61-72.
65. Youngstedt, S. D., Kline, C. E., Elliott, J. A., Zielinski, M. R., Devlin, T. M. & Moore, T. A. (2016) Circadian Phase-Shifting Effects of Bright Light, Exercise, and Bright Light + Exercise, *J Circadian Rhythms.* 14, 2.
66. Charles, A. C. & Baca, S. M. (2013) Cortical spreading depression and migraine, *Nat Rev Neurol.* 9, 637-44.
67. Wiggers, A., Ashina, H., Hadjikhani, N., Sagare, A., Zlokovic, B. V., Lauritzen, M. & Ashina, M. (2022) Brain barriers and their potential role in migraine pathophysiology, *J Headache Pain.* 23, 16.
68. Fraser, C. L. (2022) Visual Snow: Updates on Pathology, *Curr Neurol Neurosci Rep.* 22, 209-217.
69. Schankin, C. J., Maniyar, F. H., Chou, D. E., Eller, M., Sprenger, T. & Goadsby, P. J. (2020) Structural and functional footprint of visual snow syndrome, *Brain.* 143, 1106-1113.
70. Puledda, F., Schankin, C. J., O'Daly, O., Ffytche, D., Eren, O., Karsan, N., Williams, S. C. R., Zelaya, F. & Goadsby, P. J. (2021) Localised increase in regional cerebral perfusion in patients with visual snow syndrome: a pseudo-continuous arterial spin labelling study, *J Neurol Neurosurg Psychiatry.* 92, 918-926.
71. Ikeda, Ryosuke, et al. "REV-ERB α and REV-ERB β function as key factors regulating Mammalian Circadian Output." *Scientific reports* 9.1 (2019): 1-9.
72. Connolly, Emma, et al. "Prevalence of age-related macular degeneration associated genetic risk factors and 4-year progression data in the Irish population." *British Journal of Ophthalmology* 102.12 (2018): 1691-1695

73. García-Layana, Alfredo, et al. "Early and intermediate age-related macular degeneration: update and clinical review." *Clinical interventions in aging* (2017): 1579-1587.
74. Stepicheva, Nadezda A., et al. "Melatonin as the possible link between age-related retinal degeneration and the disrupted circadian rhythm in elderly." *Retinal Degenerative Diseases: Mechanisms and Experimental Therapy*. Springer International Publishing, 2019.
75. O'Leary, Fionn. "The blood-retina barrier in health and disease." (2021).
76. Raleigh, David R., et al. "Tight junction-associated MARVEL proteins MarvelD3, tricellulin, and occludin have distinct but overlapping functions." *Molecular biology of the cell* 21.7 (2010): 1200-1213.
77. Schurhoff, Nicolette, and Michal Toborek. "Circadian rhythms in the blood-brain barrier: impact on neurological disorders and stress responses." *Molecular Brain* 16.1 (2023): 1-18.
78. Oh-oka, Kyoko, et al. "Expressions of tight junction proteins Occludin and Claudin-1 are under the circadian control in the mouse large intestine: implications in intestinal permeability and susceptibility to colitis." *PloS one* 9.5 (2014): e98016.
79. Bharadwaj, Arpita S., et al. "Role of the retinal vascular endothelial cell in ocular disease." *Progress in retinal and eye research* 32 (2013): 102-180.
80. Pournaras, Constantin J., et al. "Regulation of retinal blood flow in health and disease." *Progress in retinal and eye research* 27.3 (2008): 284-330.
81. Kaur, Gaganpreet, Wendy Leskova, and Norman R. Harris. "The Endothelial Glycocalyx and Retinal Hemodynamics." *Pathophysiology* 29.4 (2022): 663-677.
82. Toda, Ryotaro, et al. "Comparison of drug permeabilities across the blood-retinal barrier, blood-aqueous humor barrier, and blood-brain barrier." *Journal of pharmaceutical sciences* 100.9 (2011): 3904-3911.
83. Parton, Robert G., and Miguel A. Del Pozo. "Caveolae as plasma membrane sensors, protectors and organizers." *Nature reviews Molecular cell biology* 14.2 (2013): 98-112.
84. Andreone, Benjamin J., et al. "Blood-brain barrier permeability is regulated by lipid transport-dependent suppression of caveolae-mediated transcytosis." *Neuron* 94.3 (2017): 581-594.
85. Hofman, Pim, et al. "VEGF-A induced hyperpermeability of blood-retinal barrier endothelium in vivo is predominantly associated with pinocytotic vesicular transport and not with formation of fenestrations." *Current eye research* 21.2 (2000): 637-645.
86. Mann, Samantha S., et al. "The symmetry of phenotype between eyes of patients with early and late bilateral age-related macular degeneration (AMD)." *Graefe's Archive for Clinical and Experimental Ophthalmology* 249 (2011): 209-214.
87. Campbell, Matthew, and Peter Humphries. "The blood-retina barrier: tight junctions and barrier modulation." *Biology and regulation of blood-tissue barriers* (2013): 70-84.
88. Acharya, Nimish K., et al. "Retinal pathology is associated with increased blood-retina barrier permeability in a diabetic and hypercholesterolaemic pig model: Beneficial effects of the LpPLA2 inhibitor Darapladib." *Diabetes and Vascular Disease Research* 14.3 (2017): 200-213.
89. Saker, S., et al. "The effect of hyperglycaemia on permeability and the expression of junctional complex molecules in human retinal and choroidal endothelial cells." *Experimental Eye Research* 121 (2014): 161-167.

90. Fan, Yichao, et al. "Exendin-4 alleviates retinal vascular leakage by protecting the blood–retinal barrier and reducing retinal vascular permeability in diabetic Goto-Kakizaki rats." *Experimental eye research* 127 (2014): 104-116.
91. Tisi, Annamaria, et al. "The impact of oxidative stress on blood-retinal barrier physiology in age-related macular degeneration." *Cells* 10.1 (2021): 64.
92. Zhao, Zhen, et al. "Establishment and dysfunction of the blood-brain barrier." *Cell* 163.5 (2015): 1064-1078.



Appendix A. The Munich Chronotype Questionnaire (MCTQ) used to calculate participants chronotype

Munich ChronoType Questionnaire (MCTQ)

Instructions:

In this questionnaire, you report on your typical sleep behaviour over the past 4 weeks. We ask about work days and work-free days separately. Please respond to the questions according to your perception of a standard week that includes your usual work days and work-free days.

Personal Data

Date: _____

Age: _____ years

Sex: female male

Height: _____ cm

Weight: _____ kg

MCTQ

I have a regular work schedule (this includes being, for example, a housewife or househusband):
Yes I work on 1 2 3 4 5 6 7 day(s) per week.
No
Is your answer "Yes, on 7 days" or "No", please consider if your sleep times may nonetheless differ between regular 'workdays' and 'weekend days' and fill out the MCTQ in this respect.



Please use 24-hour time scale (e.g. 23:00 instead of 11:00 pm)!

Workdays

Image 1: I go to bed at _____ o'clock.
Image 2: Note that some people stay awake for some time when in bed!
Image 3: I actually get ready to fall asleep at _____ o'clock.
Image 4: I need _____ minutes to fall asleep.
Image 5: I wake up at _____ o'clock.
Image 6: After _____ minutes I get up.
I use an alarm clock on workdays: Yes No
If "Yes": I regularly wake up BEFORE the alarm rings: Yes No

Free Days

Image 1: I go to bed at _____ o'clock.
Image 2: Note that some people stay awake for some time when in bed!
Image 3: I actually get ready to fall asleep at _____ o'clock.
Image 4: I need _____ minutes to fall asleep.
Image 5: I wake up at _____ o'clock.
Image 6: After _____ minutes I get up.
My wake-up time (Image 5) is due to the use of an alarm clock: Yes No
There are particular reasons why I cannot freely choose my sleep times on free days:
Yes If "Yes": Child(ren)/pet(s) Hobbies Others for example: _____
No

Work Details

In the last 3 months, I worked as a shift worker.
No Yes (please continue with "My work schedules are ...").

My usual work schedule ...
... starts at _____ o'clock.
... ends at _____ o'clock.

My work schedules are ...
... very flexible ... a little flexible ... rather inflexible ... very inflexible

I travel to work ...
... within an enclosed vehicle (e.g. car, bus, underground)
... not within an enclosed vehicle (e.g. on foot, by bike)
I work at home.

For the commute to work, I need _____ hours and _____ minutes.
For the commute from work, I need _____ hours and _____ minutes.

Stimulants

Please give approximate/average amounts!

	per → day / week / month
I smoke _____ cigarettes ...	<input type="checkbox"/> <input type="checkbox"/> <input type="checkbox"/>
I drink _____ glasses of beer ...	<input type="checkbox"/> <input type="checkbox"/> <input type="checkbox"/>
I drink _____ glasses of wine ...	<input type="checkbox"/> <input type="checkbox"/> <input type="checkbox"/>
I drink _____ glasses of liquor/whiskey/gin etc. ...	<input type="checkbox"/> <input type="checkbox"/> <input type="checkbox"/>
I drink _____ cups of coffee ...	<input type="checkbox"/> <input type="checkbox"/> <input type="checkbox"/>
I drink _____ cups of black tea ...	<input type="checkbox"/> <input type="checkbox"/> <input type="checkbox"/>
I drink _____ cans of caffeinated drinks (soft-drinks) ...	<input type="checkbox"/> <input type="checkbox"/> <input type="checkbox"/>
I take sleep medication _____ times ...	<input type="checkbox"/> <input type="checkbox"/> <input type="checkbox"/>

Time Spent Outdoors

On average, I spend the following amount of time outdoors in daylight (without a roof above my head):
on workdays: _____ hours _____ minutes
on free days: _____ hours _____ minutes



Appendix B. Participant Health Questionnaire

All information gathered will be kept secure and anything kept on computer will be password protected.

If after completing the questionnaire you have any comments or questions we are happy to discuss.

What age are you?

Have you been told you have Age Related Macular Degeneration (AMD)?

If so what year was it diagnosed?

Do you attend and eye doctor for your condition?

Do you take any supplements for AMD? (please circle)

Macushield

Macushield Gold

Lutein Omega

Macuguard

Macuguard Plus

Optivite

Other _____

Have you been told that you have other condition(s) affecting your eyes?

If you answered yes to the above question please expand:

Have you ever had eye surgery?

If you answered yes to the above question please expand:

Did you have a weak eye when you were a child?

Do you use any eye drops?

Please list the eye drops that you use:

Have you been told that you have high blood pressure?

Have you been told that you have high cholesterol?

Do you have diabetes?

If yes, when were you diagnosed?



Is your diabetes managed by: (please circle)

Lifestyle and dietary modification

Diabetes medications

Insulin

Have you had a: (please circle)

Heart attack

Stent(s) inserted

Heart surgery

Stroke

Problems with your kidneys

Recent surgery of any kind (within last three months)

If yes to any of the above, please indicate when this occurred and if you continue to be seen in hospital as a result:

Have you, or have you ever been told that you have epilepsy?

Do you have any allergies?

Do you have a shellfish allergy?

If yes, what happens when you eat shellfish?

Are you, or is there any chance that you might be pregnant at this time?

Please list all medications that you currently take and the doses. Please include supplements:

Do you, or have you ever smoked? (please circle):

Current smoker

Never smoker

Previous smoker

For how many years did you smoke for?

How many cigarettes did you smoke a day?

How often do you exercise? (please circle)

Less than half an hour, up to twice a week

Greater than half an hour, 3-4 times a week

Greater than half an hour, 5-6 times a week

Greater than half an hour, every day

Less than above options

Is there a family history of problems with sight?

If yes, which family member(s) and what problem(s) did they experience?



Is there a family history of AMD?

If yes, which family member(s)?

Is there a family history of glaucoma?

If yes, which family member(s)?

Is there a family history of cataracts?

If yes, which family member(s)?

Which ethnicity are you? (please circle)

Caucasian

Asian

African

Hispanic

Other _____